Università degli Studi di Cagliari

PhD DEGREE

in

Life, Environmental and Drug Sciences Biomedical Curriculum

XXXIII Cycle

Defects in genes involved in heme biosynthesis: first molecular step for the development of potential salivary biomarkers correlated with porphyrias

BIO/10

PhD Student: ***Doctor Stefania Solinas***

Supervisors ***Professor Alessandra Padiglia***

Professor Tiziana Cabras

Final exam academic year 2019 – 2020

Thesis defence: April 2021 Session

Contents

Abstract

Heme is an important molecule involved in several biological processes such as oxygen transport and its storage in myocytes as a component of the respiratory proteins haemoglobin and myoglobin. Moreover, heme is a component of various other haemoproteins such as cytochromes, catalase, peroxidase, tryptophan pyrroles, and nitric oxide synthase. Heme plays a role in the pathogenesis of diseases, in fact defects in any enzyme of the pathway may cause porphyric disorders.

Porphyrias are a group of metabolic and genetic diseases characterized by a deficiency in the activity of specific enzymes in the heme pathway.

The abnormal function of one of the eight enzymes involved in this pathway, has as a result eight different types of porphyria that lead to accumulation of pathway intermediates.

Porphyrias are divided in acute porphyrias which included autosomal dominant porphyrias such as Acute Intermittent Porphyria (AIP), Variegated Porphyria (VP), Hereditary Coproporphyria (HCP) and a rare autosomal recessive porphyria 5-Aminolevulinc Acid Dehydratase deficiency Porphyria (ALADP); and non-acute or cutaneous porphyrias that included Congenital Erythropoietic Porphyria (CEP), Porphyria Cutanea Tarda (PCT), Erythropoietic Protoporphyria (EPP) and X-Linked Protoporphyria (XLP).

In the first part of this thesis, we have conducted molecular studies on DNA extracted from saliva and blood samples obtained from Italian and Spaniard patients. The analysis conducted on the CPOX and FECH gene of an Italian patient affected by VP, revealed some polymorphisms not directly associated with the patient phenotype. Numerous nucleotides present in heterozygosity and an insertion of six nucleotides, (18505_6insTATTCT), were found in the 3' UTR region of the CPOX gene, which is an important region for the half-life of the messenger. Analysis of the PPOX gene have shown frameshift mutations between exons 2 and 3 (c.5710_5711ins.CG, c.5714_5715ins.A,

c.5720_5721ins.CT), which led on a stop signal in exon 4. Results obtained at Hospital Universitario 12 de Octubre (Madrid, Spain) confirmed two new mutations in Spaniard patients with AIP: Ivs11+3A>T in intron 11 and c.41_42ins.A in exon 3.

In the second part we analyzed porphyrin intermediates in body biofluids (blood, urine and faeces) in patients with suspected porphyria. In particular, we quantified, by micro chromatography and spectrophotometry, the presence of these metabolites in patients diagnosed with porphyria. The results obtained showed that porphyrin precursor concentrations were particularly high in urine and faeces during acute porphyria attacks and also in blood in patients with cutaneous porphyrias when exposed to sunlight.

In the third part we focused on the quantitative and qualitative proteomic study of proteins present in saliva of porphyric patients. Proteomics is a valid investigation tool in the search for biomarkers in specific pathologies. In patients with cutaneous porphyria skin lesions, caused by porphyrin precursors that are activated by exposure to the sun in parts of the body such as the face, affecting also the oral cavity, creating serious lesions to the oral mucosa. The accumulation of these precursors may also cause a brownish teeth discoloration. The salivary study of these patients aims to identify specific biomarkers for the diagnosis of different types of porphyria, through the use of bottom-up approach based on SDS-PAGE technique used for the separation of the proteins. After the separation of the proteins, followed the in-gel trypsin digestion and the characterization of proteins by high-resolution mass-spectrometry. We created 3 separate saliva pools for patients with porphyria, divided into: Pool 1 for IAP patients, Pool 2 for VP patients and Pool 3 for HCP patients, and 1 saliva pool from healthy subjects with the same sex-age ratio as patients and the same final concentration.

Unfortunately, due to the Covid-19 emergency, the results are still being processed.

Introduction

1 Heme

Heme is an important molecule involved in several biological processes such as oxygen transport or its storage in myocytes as a component of the respiratory proteins haemoglobin and myoglobin. Moreover, heme is a component of various other haemoproteins[1] such as cytochromes, catalase, peroxidase, tryptophan pyrroles, and nitric oxide synthase. Structurally, the biological molecule, named ferroprotoporphyrin IX, consists of a tetrapyrrole ring, an organic complex structure containing an atom of ferrous iron (Fe^{2+}) in its centre. This ferrous iron atom (Fe^{2+}) presents six electron pairs, four of which are bonded to the pyrrolic nitrogen of the porphyrin macrocycle, while of the other two electron pairs, which are perpendicular to the porphyrin plane, one is bonded to a histidine residue of the globin chains and one is bonded to the oxygen[2].

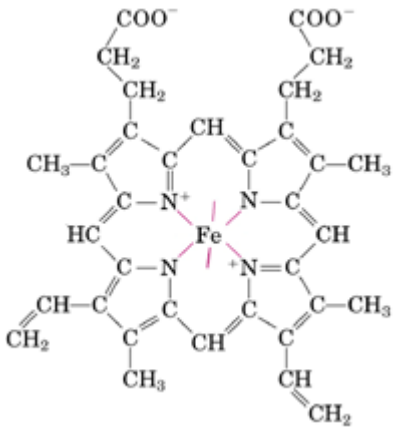

Figure 1. *Heme structure.*

Heme is produced in each human cell for oxidation-reduction and respiratory reactions, and especially in erythropoietic cell for haemoglobin synthesis and in the liver parenchymal cells with the purpose of forming the prosthetic group of cytochromes and haemoproteins[2].

Most of the heme is synthesized by the bone marrow for about 80% for the synthesis of haemoglobin, while the remaining 20% is synthesized by the liver, where it is mainly used for the production of cytochrome P450, which regulates its production by 5-aminolevulinate synthase 1 (ALAS1).

1.1 Heme pathway

The biosynthetic pathway of heme (figure 3) first occurs in the mitochondria, followed by three cytoplasmic steps and concludes the final stages of its formation anew in the mitochondria[2].

All tetrapyrroles, such as heme, are synthesized starting from a common precursor δ-aminolaevulinic acid (ALA).

The first reaction is catalysed by δ-aminolaevulinic synthase (ALA synthase or ALAS). As regard the catalytic strategy, the bond between glycine and pyridoxal phosphate activates the α carbon of glycine, which performs an attack on the thioester carbon of succinyl-CoA, then occurs a decarboxylation with the consequent formation of 5-aminolevulinc acid ALA in the mitochondrial matrix (figure 2).

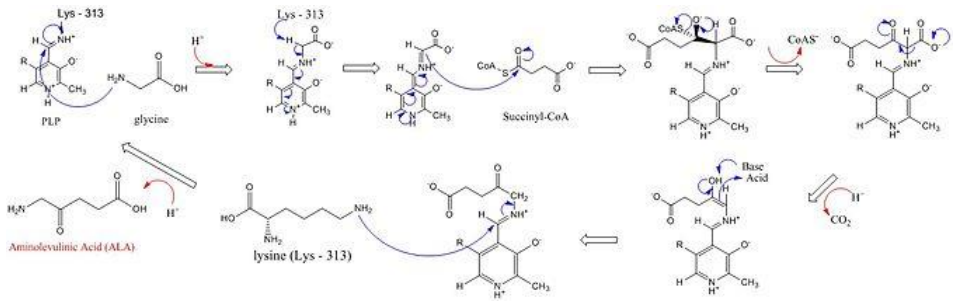

Figure 2. *Catalytic strategy and formation of 5-aminolevulinic acid ALA*

ALA is exported in the cytosol, and the enzyme ALA-dehydratase catalyses the subsequent reaction during which two molecules of ALA condense forming the monopyrrole porphobilinogen (PBG).

Four porphobilinogen molecules combine in a deaminase-mediated reaction join by hydroxymethylbilane synthase (HMBS), resulting in the first tetrapyrrole compound, uroporphyrinogen III[3].

Two enzymes play a role during this reaction: the first is uroporphyrinogen I synthase (UROS), which leads to the formation of a not-desired symmetrical compound; the second is the uroporphyrinogen III co-synthase, which allows the oscillation of one of the pyrrole rings forming uroporphyrinogen III, an asymmetric tetracyclic compound.

Uroporphyrinogen III undergoes a decarboxylation of acetic acid side chains by uroporphyrinogen decarboxylase (UROD) to form coproporphyrinogen III.

Coproporphyrinogen returns to the mitochondria where it is oxidatively decarboxylated by coproporphyrinogen oxidase (CPOX) to obtain protoporphyrin IX by the enzyme protoporphyrinogen oxidate (PPOX).

The last reaction is catalysed by the ferrochelatase enzyme (FECH) which inserts ferrous iron into protoporphyrin IX to form heme.[4]

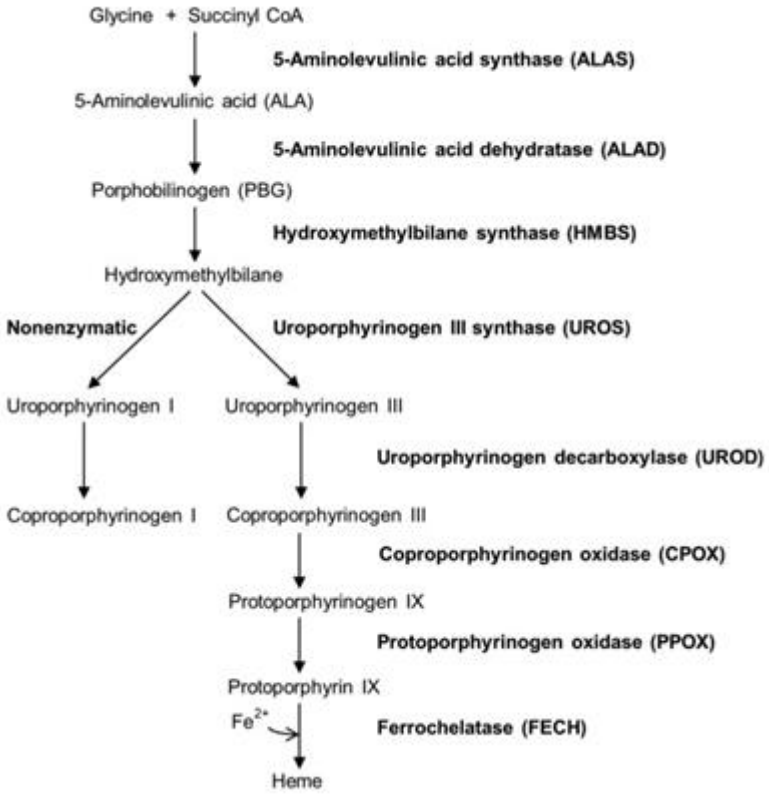

Figure 3. *Scheme of heme biosynthetic pathway.*

Heme plays a role in the pathogenesis of diseases, in fact defects in any enzyme of the pathway may cause a porphyric disorder[1].

2 Porphyrias

Porphyrias are a group of metabolic and genetic diseases characterized by a deficiency in the activity of specific enzymes in the heme pathway. This disease takes its name from the Greek word "πορφύρα" for the red colour of the urine[5]. The abnormal function of one of the eight enzymes involved in this pathway, has as a result eight different types of porphyria that lead to accumulation of pathway intermediates.

Porphyrias are divided, due to their clinical manifestations, into groups: acute and non-acute, and/or hepatic and erythropoietic porphyrias[2]. Acute porphyrias are inborn errors which included autosomal dominant porphyrias: Acute Intermittent Porphyria (AIP), Variegated Porphyria (VP), Hereditary Coproporphyria (HCP) and a rare autosomal recessive porphyria 5-Aminolevulinc Acid Dehydratase deficiency Porphyria (ALADP)[6]. These porphyrias are accompanied by severe abdominal, psychiatric, neurological and cardiovascular symptoms.

Non-acute porphyrias included Congenital Erythropoietic Porphyria (CEP), Porphyria Cutanea Tarda (PCT), Erythropoietic Protoporphyria (EPP) and X-Linked Protoporphyria (XLP). These porphyrias showed an accumulation of porphyrins in the skin and in the liver with consequent photosensitivity and possible liver damage. These porphyrins, after exposure to sunlight (visible spectrum, including near ultraviolet [UV] lights), generated cytotoxic radicals that caused recurrent or persistent skin manifestations. Phototoxic protoporphyrins in patients with EPP, are activated in the superficial vessels by blue light with consequently production of free radicals that lead to severe neuropathic pain lasting hours or days and starting 1 to 20 minutes after sun exposure[7].

2.1 Acute intermittent porphyria

Acute Intermittent Porphyria (AIP) is a metabolic disorder inherited as an autosomal dominant pattern with variable penetrance. AIP is the most common form of acute hepatic porphyria. This type of porphyria is due to mutations of PBGD (or hydroxymethylbilane synthase HMBS), which is the third enzyme of the heme synthesis pathway. PBGD has a structure of about 40 kDa[8] divided into three domains: in humans, domain 1 and 2 comprised five beta-sheets and three alpha-helices, while domain 3, which is located between the other two, has a flattened beta-sheet.

A dipyrromethene cofactor (DPM cofactor) at the active site, consists of two condensed PBG molecules, covalently bound to domain 3. This molecule is located in a deep cleft between domains

1 and 2 (figure 4). Positively charged arginine residues, near the active site, have been shown to stabilize the carboxylated functionalities on the incoming PBG and the growing pyrrole chain, which presumably promote the formation of the final hydroxymethylbilane (HMB) product. PBGD exists in dimer units in the cell cytoplasm. This structure is highly conserved in organisms[9].

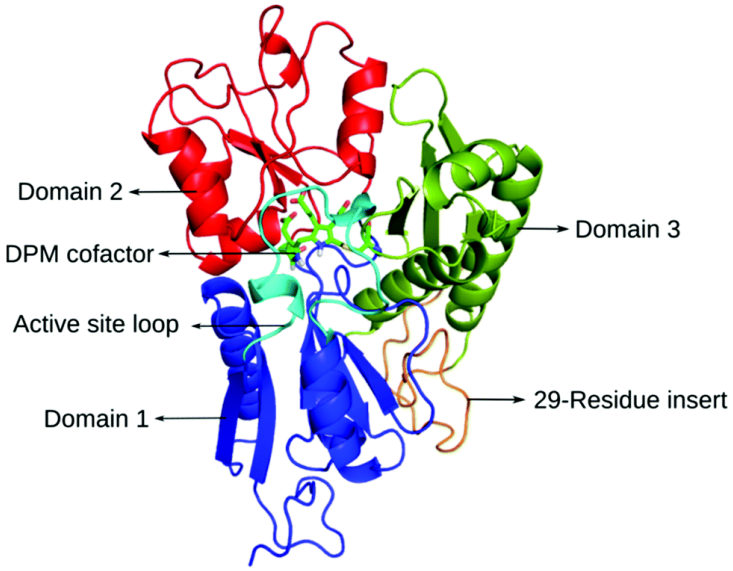

Figure 4. *α-helix and β-sheet structure of porphobilinogen deaminase domains.*

PBGD gene is extended about 10 kb on chromosome 11q23[10] (figure 5), and contains 15 exons and 14 introns.

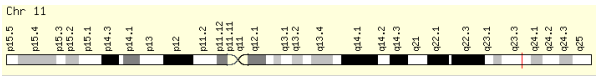

Figure 5. *PBGD gene genomic location. Chromosome 11q23.*

This gene is encoded by two different mRNAs expressed in a tissue-specific way: a transcription occurs in erythroid tissues[11] by a specific promoter located 3 kb from exon 1 that encodes exon 2 through 15[12]; the housekeeping transcription is expressed in all tissues[11] by a specific promoter 5' to produce mRNA that encodes exon 1 and 3 to 15[12]. Mutations in this gene, showing a deficiency

of enzymatic function of about 50%, especially in hepatocyte and are not directly related to disease severity in fact, despite its hereditary transmission, most of heterozygous genotype do not manifest symptoms of the disease[13].

AIP leads to hepatic over production of upstream neurotoxic heme precursors PBG and δ-aminolaevulinic acid (ALA). The overproduction of these hepatic hemoproteins induces massive heme synthesis and the rate-limiting of ALAS is induced, in the liver, by increasing the production of ALA and PBG, the PBGD substrate[11].

Concentrations increasing depend on several factors that can activate hepatic heme synthesis for example infections, lead poisoning, pharmacotherapies such as barbiturates or sulphonamides, drugs abuse such as alcohol and tobacco, and hormonal changes such as during the menstrual cycle (in fact female are more affected than male). Symptoms appear generally after puberty during the third to fourth decade of life but homozygous genotype, less common, develop neurological symptoms since childhood.[10] Patients with AIP manifest both asymptomatic periods and acute visceral and neurological attacks showing high ALA and PBG blood and urinary levels that increase during acute attacks. Porphyrin precursors ALA and PBG are colourless but during PBG degradation, its oxidation forms PBG which is a dark coloured pigment that leads to the deep red urine, important in the diagnosis.[13]

2.2 Variegated porphyria

Variegated Porphyria (VP) is an autosomal dominant inherited trait with reduced penetrance, caused by a deficit in protoporphyrinogen oxidase (PPOX) activity.[14] VP has a high frequency in South Africa, presumably they are all descended from a couple from the Netherlands who married in Cape in 1688[12] , but can be found all over the world.

PPOX, the penultimate enzyme of the heme biosynthetic pathway, is a homodimeric flavoprotein that catalyses the oxygen dependent aromatization of protoporphyrinogen into protoporphyrinogen IX (PPO)[15].

Human PPOX has a structure of about 51 kDa (477 amino acids). The enzyme is located on the inner membrane of mitochondria; its N-terminal region contains a conserved sequence (G-X-G-X-X-G-) which is a dinucleotide binding site typical of many flavoproteins[16]. The pathway of its targeting into the inner mitochondrial membrane and its import is unknown[15]. PPOX is synthesized as the same transcript both in erythroid and non-erythroid cells[16].

Mutations in PPOX gene can produce a non-functional enzyme, or a poorly functional enzyme (approximately 50% less of activity)[14]. South African VP families present the same mutation (R59W) that is close to the flavin cofactor binding[12].

PPOX gene is extended about 8 kb on chromosome 1q22 (figure 6) and contains 13 exons and 12 introns.

Figure 6. *PPOX gene genomic location. Chromosome 1q22.*

Exon 1 is formed by a 5' untranslated region ending in exon 2, which contains the first 29 amino acids residues, while exon 13 contains the carboxy-terminal domain and the 3'untraslated region[16]. VP presents both as cutaneous porphyria, with photosensitive skin, and as acute porphyria with neurovisceral symptoms, its name "variegate" derives precisely for its different clinical manifestations[17]. Skin lesions appear, in sun-exposed skin especially in hands and face, as subepidermal blisters but other severe skin damage may occur such as milia, scarring, thickening, hypertrichosis and hyperpigmentation[14]. Acute symptoms appear, after puberty and are more

common in female, as abdominal pain, constipation, colicky, nausea, vomiting, hypertension, pain in the back, chest, and extremities, anxiety, seizures and, in severe cases, motor neuropathy which can lead to tetra paresis and respiratory paralysis[14].

As for AIP, also in VP the increase in the concentration of porphyrin products depends on several porphyrinogenic factors such as alcohol abuse, cigarettes, drugs, barbiturates, hormonal changes, infections and dieting[18].

2.3 Hereditary Coproporphyria

Hereditary Coproporphyria (HCP), the least common of the acute porphyrias[12], is an autosomal dominant disorder inherited with low penetrance[19]. As AIP and VP, HCP is the result of a partial deficiency (50%) in the enzymatic activity of coproporphyrinogen oxidase (CPOX), which derives from the expression of the normal gene allelic to the mutant gene[12]. CPOX, the sixth enzyme in the heme pathway, is a homodimer that catalyzes the conversion of coproporphyrinogen III (CPO) to PPO and is situated in the inner mitochondrial membrane [20]. During this conversion a carboxylic intermediate is formed: harderoporphyrinogen which causes a rare variant form of HCP called harderoporphyria [21]. Human CPOX gene is located on chromosome 3q11.2 (figure 7) and contains 7 exons and 6 introns.

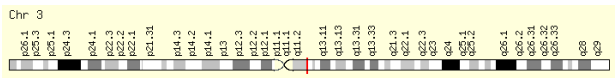

Figure 7. *CPOX gene genomic location. Chromosome 3q11.2*

CPOX encodes a precursor of 40 kDa (454 amino acids)[20], that contains an N-terminal amino acid residue which represents an important mitochondrial target sequence[22]. It is known that some

amino acids (four histidines) are well conserved during evolution, which suggests some importance in the function of the protein[22].

A single mutation, that replacing a lysine with a glutamic acid at position 404 (K404E), has been reported to be the cause of the harderoporphyria. Mutations in the CPOX gene lead to the accumulation of porphyrin metabolites which are normally formed during heme synthesis. Due to the reduced functionality of about 50% of the enzyme, they are accumulated becoming toxic for the organism[23].

Clinical symptoms, as in other acute porphyrias, generally appear after puberty. The most common symptoms are related to neurovisceral attacks, similar to those of AIP, and to skin fragility and bullous eruptions in sun-exposed skin, similar to those of VP[24]. Due to this duality in symptoms, HCP and VP are also called mixed porphyria[25]. During acute crises there is an increase in the production and excretion of porphyrin metabolites in urine and faeces[24]. Other causes that can contribute to the onset of symptoms of the disease are, as in other acute porphyrias, alcohol abuse, cigarettes, drugs, barbiturates, hormonal changes, infections and dieting[18].

2.4 5-Aminolevulinc acid dehydratase deficiency porphyria

5-Aminolevulinc acid dehydratase deficiency porphyria (ALADP), also known as Doss porphyria (or plumboporphyria), was identified for the first time in 1979[26]. For its capacity to inhibit ALA dehydratase and for its clinically symptoms mimics of lead poisoning[5], this is a rare form of acute porphyria of which very few cases are known worldwide[17]. Only 8 cases, all males, have been attributed to this type of porphyria of which 2 identified at birth, one at the age of 7, four at the age of 12-15 and one at the age of 63[5]. ALADP is the only acute porphyrias to be inherited as an autosomal recessive trait[27] and it is caused by a deficiency in ALAD, the second enzyme of the heme pathway, that catalyses the condensation of two ALA molecules to form a monopyrrole PBG[5].

Human ALAD is a zinc metalloenzyme of about 280 kDa composed of eight identical subunits of about 37 kDa that containing zinc atom: four of which are involved in the enzyme catalytic activity and the other four are involved in the stability of the homo-octamer structure of the protein. The zinc binding domain of the enzyme is highly conserved between species[27]. Human ALAD gene is located on chromosome 9q32 (figure 8) and consists in two non-encoding exons (1A and 1B) which produce two different mRNAs in erythroid and housekeeping cells, and 11 exons (from 2 to 12) and 12 introns spread on 13 kb DNA[12].

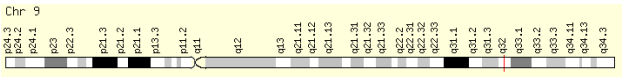

***Figure 8**. ALAD gene genomic location. Chromosome 9q32*

Mutations in ALAD can be caused both neurovisceral and neurological symptoms that included: abdominal pain, constipation, nausea, vomiting, delirium, hallucinations, anxiety, disorientation , depression[5].

2.5 Congenital Erythropoietic Porphyria

Congenital Erythropoietic Porphyria (CEP), is part of the cutaneous (or non-acute) porphyrias, and is also known as Gunther's disease[28]. Gunther, the first researcher who described this porphyria in 1911, discovered the uroporphyrinogen III co-synthase (UROS) deficiency, the fourth enzyme in heme biosynthesis that leads on accumulation of the HMB that is not transformed in uroporphyrinogen I[29]. CEP is a rare form of autosomal recessive porphyria with around 200 cases worldwide[29].

Human UROS gene is located on chromosome 10q26.2 (figure9) which spans about 37 kb DNA segment and contains 10 exons of which two are non-coding (1 and 2A) and 9 are coding exons (from 2B to 10) and 9 introns.

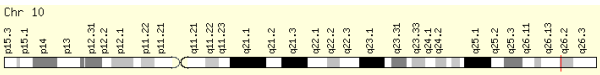

Figure 9. *UROS gene genomic location. Chromosome 10q26.2*

Exons 1 and 2A are promoters: respectively one is a housekeeping promoter while the other is an erythroid-specific promoter[30]. These promoters produce two different transcripts: the housekeeping transcript, present in all tissues and cells, contains the 5' untranslated exon that codes exons from 2B to 10; the erythroid-specific transcript, presents in fetal and adult erythropoietic tissues, contains the 5'-untranslated exon 2A that codes exons from 2B to 10. Both housekeeping and erythroid promoters have the same start codon that is located on exon 2B[30].

Deficiencies in UROS may cause skin photosensitivity in sun-exposed areas of the body. The clinical manifestations have, as a symptom, the appearance of bullae and vesicles whose rupture can lead to infections that can worsen creating deep lesions to the face and hands. Other common symptoms in Gunther's disease are hypertrichosis and skin hyperpigmentation[17]. The overproduction of porphyrin metabolites is reflected not only in bones but also in teeth, which become brownish. For all these characteristics, hypertrichosis on the face and hands, the brown teeth and for not being able to expose themselves to the sun, at these patients is attributed the werewolf legend[17].

2.6 Porphyria Cutanea tarda

Porphyria Cutanea Tarda (PCT), the most common of the porphyrias[17], is classified as a cutaneous or non-acute porphyria and is divided into two subtypes: type I PTC also known as sporadic (80% of cases worldwide)[31], and type II PCT also known as familial (20% of cases worldwide)[31], which is inherited as autosomal dominant trait with low penetrance[12]. PTC is due to the reduced activity of uroporphyrinogen decarboxylase (UROD), the fifth enzyme in the heme pathway, with a consequent enhancement of the circulating porphyrins[31].

UROD converts the URO to CPO by sequential decarboxylation of the four acetic acid substitutes[32]. The coding gene is located on chromosome 1p34 (figure 10) which spans on about 3.7 kb DNA region. Human UROD enzyme is a homodimer part of the (α/β) barrel family of 41 kDa (367 amino acid) polypeptide cytosolic enzyme without tissue-specific isoenzymes[32], that contains 10 exons and 9 introns , a single promoter , and a polyadenylation signal (AATAAA element)[33].

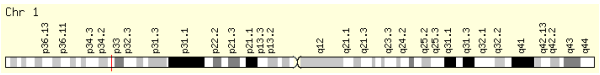

Figure 10. *UROD gene genomic location. Chromosome 1p34*

The reduced activity of the UROD enzyme to 50% respect to the normal isoform in the hepatocytes of affected patients, leads to an accumulation of uroporphyrins which pour out into the circulation and are then excreted in the urine[32]. These accumulated uroporphyrins in the cytosol are oxidated by iron and oxidative stressors. A non-partial oxidation of these metabolites may produce a molecule of uroporphomethene that can bind the enzyme but prevents, as a UROD competitive inhibitor, the metabolization as a substrate[31].

Factors such as estrogens, alcohol, iron, and diseases such as hepatitis C, or viral infections in general, can induce PCT in susceptible individuals, while part of this predisposition is due to

inheritance[12]. The most common symptoms of this pathology are cutaneous, including the appearance of vesicles and bullae in sun-exposed areas such as face, neck and hands, which evolve into crust with consequent infections. Other manifestations are excessive hair growth, scaring, thickening and skin hyperpigmentation[17]. Symptoms generally appear in the 5th or 6th decade of life and are more frequent in male[31].

2.7 Erythropoietic Protoporphyria

Erythropoietic Protoporphyria (EPP), described in 1961, is a cutaneous or non-acute porphyria caused by a mutation in ferrochelatase (FECH), the final enzyme in heme biosynthesis, which adds Fe^{+2} to protoporphyrin IX (PPIX) ring to produce heme[34]. FECH is situated in the inner mitochondrial membrane[35]. EPP is a genetic photodermatose pathology , the third most common porphyria, and is inherited as an autosomal dominant trait with low penetrance[34]. Human FECH is located on chromosome 18q21.3 (figure 11) and contains 11 exons and 10 introns[36] spans 45 kb[12] with an open reading frame of about 1269 bp.

Figure 11. *FECH gene genomic location. Chromosome 18q21.3*

Human FECH gene encodes for a precursor of 423 amino acids of which 54 are the presumed mitochondrial leader sequence[37]. FECH consists in two transcripts that produce two mRNAs diverse in 3' untranslated region length and a single promoter for the housekeeping and erythroid cells[37]. There is an alternative splice site located in exon 2, that produces an isoform with 6 extra amino acid residues[12]. The secondary structure of this protein consists in a 17 α-helices, 8 β-sheets, 2 active sites and 4 iron-sulphur cluster binding site[36].

Mutations in FECH gene may cause an enzymatic deficiency that leads on the accumulation of porphyrin metabolites both in the blood and in tissues, such as the liver and skin. In the skin it causes cutaneous manifestations that, unlike other cutaneous porphyrias, are more serious and appear as soon as the affected subjects are exposed to UV light[17]. Common skin manifestations, that start in early infancy, including redness, swelling and burning during or shortly after sun exposure, loss of lunulae of nails and the duration of pain of the skin may persist for hours and, in severe cases, several days; vesicles or bullae are inusual[38]. This type of porphyria may affect both males and females[34].

2.8 X-Linked Protoporphyria

X-Linked Porphyria (XLP) is a rare porphyria caused by a gain-of-function mutation in δ-aminolaevulinic acid synthase 2 gene (ALAS2)[39]. ALAS, the first enzyme in erythroid heme pathway[40], exists in two isoenzymatic forms: one form (ALAS1) is ubiquitous and is expressed in housekeeping cells, and is mapped to chromosome 3p21, while the other isoenzyme (ALAS2) is specific for erythroid cells, and it is mapped to chromosome Xp11.21[41] (figure 12).

Figure 12. *ALAS2 gene genomic location. Chromosome Xp11.21*

X-linked protoporphyria is inherited as an X-linked trait, is 100% penetrant in males, while in heterozygous females the variability depends on the random X-chromosome inactivation[42]. Mutations, observed only in exon 11 that encodes the C-terminus (that interact with the active site of the enzyme to regulate its activity), cause a stop or a frameshift leading to a prematurely

truncated wild-type enzyme. ALAS2 contains 587 amino acid residues which includes a transit peptide of approximately 49 amino acids[42].

ALAS2 plays a regulatory role in rate of erythroid heme pathway. Mutations in this gene can lead to an increase in the enzymatic activity of ALAS2 in a manner that insertion of iron into protoporphyrin is rate limiting for heme synthesis with consequent accumulation of metal-free and zinc-bound protoporphyrin IX[43]. The accumulated metabolites of protoporphyrin are released from the bone marrow into circulating erythrocytes and plasma and absorbed by the liver, vascular endothelium, reaching the superficial skin vascular system[39]. Protoporphyrins are activated by sunlight exposure, leading a production of singlet oxygen radical reactions with a tissue damage and pain in sun-exposed areas[39]. Symptoms of XLP, usually beginning in early infancy, include itching and burning sensation of the skin after a few minutes of sun exposure, as in patients with EPP, pain of the skin may persist for hours or days. In severe cases a marked increase in protoporphyrin levels may enhance the risk of liver dysfunction. The prevalence of this porphyria is unknown[42].

3 Human saliva

Human saliva, in physiological conditions, is a clear coloured and slightly acid body fluid complex secreted mainly by three different major glands: the parotid glands, the submandibular glands and the sublingual glands and by various minor glands[44]. These glands are regulated by the autonomic nervous system and gastrointestinal hormones, and consequently salivary efficiency, in volume and composition, changes according to the differential activation of these glands under different stimuli. Major glands emit more saliva then minor, but minor glands are more important in composition because they contribute to the protection of the oral cavity.

Saliva is also formed by desquamated cells of the mucosa and by the crevicular gingival fluid which contains oral bacterial and food residues. This type of fluid is called “whole saliva”, while is used the

generic term “saliva” referring to that secreted by glands[45].

Glands contribute in different percentages to salivary flow. Normally, in healthy and unstimulated, the amount of salivary flow is between 1 and 1.5 L per day and about 20% originates from the parotid glands, 65% from submandibular glands, 8% from the sublingual glands and the remaining 10% from the minor glands. If these glands are stimulated, the percentages completely change and the contribute of the parotid glands are more than 50% of total salivary secretion.

Saliva is involved in multiple functions that affect oral health such as protect oral tissues, create a balance for teeth remineralisation, antimicrobial activity creating a barrier against bacterial, digestion and taste perception. Another important function is the lubrification of oral cavity, induced by mucins (excreted by minor glands), that supports a correct mastication, speech and swallowing.

4 Human blood

Human blood is a dense fluid that contains several elements, including platelets, leukocytes and mainly erythrocytes in an aqueous polymer solution called plasma[46]. Blood behaves like a non-Newtonian fluid and its rheology is given by the hematocrit, the aggregation and mechanics of the red cells and the viscosity of the plasma[47]. Blood cells are formed during a process called hematopoiesis, which occurs in the bone marrow presents in the diaphysis of long bones and in the pores of cancellous bone and lymphoid tissue. In the human body, metabolic communication occurs through the blood as it carries nutrients, oxygen, hormones, ions etc[48]. The volume of blood presents in an adult individual is about 5-6 liters, half of which is composed of red cells or erythrocytes, and to a lesser extent white cells or leukocytes and platelets[48]. Plasma consists of 90% water and 10% of dissolved substances, of which 70% is formed by plasma proteins, 20% by organic metabolites and 10% by inorganic salts[48].

5 Human urine

The kidneys have an active respiratory metabolism and can use free fatty acids, ketone bodies, amino acids and blood glucose as an energy source, degrading them, when the Krebs cycle is completed, obtaining, through oxidative phosphorylation, energy in the form of ATP[48]. Most of this energy is used to produce urine, an aqueous solution consisting mainly of electrolytes and excretory metabolic products formed by the kidneys[49]. Urine formation occurs in steps: all the plasma components, except for proteins and lipids, are filtered by the glomerulus, present in the kidney cortex, and then moved into the renal tubules which absorb ions and metabolites and then transfer them to the blood[48]. During the passage of the filtered plasma, water is also absorbed thanks to vasopressin hormone produced by the pituitary gland, varying the composition and concentration of the glomerular filtrate as it proceeds along the tubules. 1 mL of final urine is formed by the concentration of a volume ranging from 50 to 100 mL of glomerular filtrate. The urine components change according to hydration and diet and are important for its characterization[48]. Example of components: glucose, ions, and metabolic waste products such as urea, uric acid and creatinine. The characteristics of the urine reflect the health of a patient since color, smell and pH can vary. The color of the urine reflects the concentration of its components: if the urine appears cloudy it may be due to the presence of bacteria, white blood cells, red blood cells or epithelial cells. Urine is normally a clear and odorless fluid but depending on age, it can acquire an aromatic odor based on the decomposition of its components, even some foods can alter its smell. Urine pH is used as an indicator of the kidney's ability to eliminate toxic substances, it can change during the day, decreasing in the early morning and increasing in the evening[49].

6 Aim of the work

This thesis project is focused on the analysis of nucleic acids, enzymes, porphyrin intermediates and proteins involved in the heme biosynthetic pathway.

The purpose of part 1 of this thesis was to use genomic DNA to define, through Polymerase Chain Reaction (PCR) technique, the presence of new and already classified mutations, to attribute the correct genotype to patients affected by different types of porphyrias and to conduct familiar studies.

The aim in part 2 was to analyze porphyrin intermediates in body biofluids (blood, urine and faeces) in patients with suspected porphyria and to quantify, by micro chromatography and spectrophotometry, the presence of these metabolites in patients diagnosed with porphyria.

The part 3 was focused on the quantitative and qualitative proteomic study of proteins present in saliva of patients with all forms of porphyria in order to identify new potentially salivary biomarkers, which could be helpful in both diagnosis and classification of the different forms of porphyria.

My research activity was performed partly during my abroad period project at the Hospital Universitario 12 de Octubre (Madrid, Spain) under the supervision of Professor Rafael Enriquez de Salamanca and doctor Javier Castelbon, and partly at the University of Cagliari under the supervision of Professor Alessandra Padiglia.

7 Vampires, Werewolves, Kings and Porphyria

Clinical manifestations, in patients with porphyria, are due to the accumulation of porphyrin intermediates that can cause deformations in sun-exposed areas of the body, and for these reasons have inspired the myth of vampires[50]*. In 1885 Emily Gerard, in her book "Transylvanian Superstitions", describes a demonic creature that drank human blood and according to superstitions, the only way to kill these creatures was using a stake. The vampire myth becomes more popular with "Count Dracula", who first appeared in Bram Stoker's novel in 1897. Dracula avoids sun exposure, has protruding teeth and, despite being an imaginary character, has some characteristics in common with patients with PCT. For example, in some patients, the skin around the mouth shrinks due to sun damage and as a result shows teeth that appear more prominent, moreover avoiding the sun, they have a pale skin complexion that physically resembles a vampire*[51]*. Patients with congenital erythropoietic porphyria, a rare form of porphyria, have features in common with werewolves in that they develop hypertrichosis and hyperpigmentation on the face and body and deformation of the nails and hands, in addition to characteristic skin lesions*[52]*.*

It is assumed that King George III's madness was also due to frequent attacks of porphyria. In addition to the genetic predisposition, phenotypically correlated with VP, his symptoms were amplified by heavy metal poisoning[53]*.*

PART 1:

MOLECULAR ANALYSIS OF GENES INVOLVED IN HEME BIOSYNTHESIS PATHWAY FROM PORPHYRIC PATIENTS

1 Human saliva in molecular research

Currently, different techniques are applied to the detection and quantification of salivary biomarkers such as polymerase chain reaction (PCR), mass spectrometry (MS), immunoassay or enzymatic techniques, microarrays etc. These techniques are feasible because saliva is rich in DNA (present in the flaking cells of the buccal mucosa), proteins (more than 3000) and peptides (more the 12000)[54].

Saliva is an important matrix that offers the opportunity to carry out various strategies of investigation due to its simple and non-invasive collection, compared with other biofluids such as blood. In fact, one of the advantages of collecting saliva samples, as an alternative to blood samples, is their stability at room temperature and the large amount that can be requested from the donors with a minimal invasive way, while disadvantages include potential bacterial DNA contamination and lower average DNA yield. The yield may depend on several factors that preceding sample collection, e.g. the change in the contents of the mouth or by the DNA extraction method[55].

In biomedical research, the isolation of nucleic acids DNA and RNA is the crucial point of the molecular techniques, and their extraction can also be performed from saliva samples, obtaining good quality. DNA extracted from salivary samples, has proven to be an adequate template used for molecular investigations involving the detection of both germline mutations and single nucleotide polymorphisms (SNPs)[55].

2 Human Blood in molecular analysis

The importance of using blood in biochemistry, hematology, clinical studies and forensic investigations is due to because it is an important source of genomic DNA for to the presence of nucleated white blood cells[56]. Through a blood test it is possible to acquire precise and updated information on specific diseases and may also open new opportunities for faster, less invasive and

more convenient diagnosis and prediction of molecularly targeted treatments on individualized sampling and molecular stratification.

Many protocols and different techniques can be used for extracting DNA or RNAs from whole blood, by commercial kits, more or less expensive, from which good yield and quality can be obtained.

MATERIALS AND METHODS

3 DNA extraction from saliva

Genomic DNA of selected subjects was extracted from buccal cavity cells present in saliva. For each subject, approximately 1 mL of saliva was collected in sterile 1.5 mL tubes. The biological sample was stored at a temperature of 4 °C before the use. The DNA was purified from the cells using commercial GeneMATRIX Tissue DNA Purification Kit (EURX Ltd, Poland), following an experimental protocol provided by the manufacturer.

After centrifugation at 12000 rpm for 10', the supernatant was removed and the pellet containing the cells was resuspended by vortex with the auxiliary of 200 µL of "Lyse T" buffer (containing sodium dodecyl sulphate) and 2 µL of RNase A. Then, the sample was incubated for 5'at room temperature and subsequently treated with 10 µL of Proteinase K and 200 µL of "Sol T" buffer and incubated at 70 °C for 10'. After the incubation period, the sample was mixed with 200 µL of 96% ethanol, then centrifuged for 1' at 12000 rpm in order to settle the contaminating macromolecules present in the lysate. The supernatant, containing the nucleic acids, was transferred onto the adsorption chromatographic column, previously equilibrated with the "buffer T", and centrifugated for 1' at 12000 rpm. The DNA, bound to the silica membrane, was subjected to two series of washes, respectively with the buffers "Wash TX1" and "Wash TX2" containing ethanol. The last step of the

extraction allows the elution of the DNA from the column through the use of a solution containing 5 mM Tris-HCl, solution able to promote the release of DNA from the fixed phase of the column. The DNA was then stored in a sterile test tube. The concentration and purity of the DNA was determined spectrophotometrically using Nanodrop technology, by measuring respectively the absorbance at 260 nm (A 260) and the ratio between the absorbance values at 260 nm and 280 nm (A 260/280).

3.1 DNA extraction from blood

Genomic DNA was purified from blood using commercial NZY Blood gDNA isolation Kit (NZYTECH, Portugal) following an experimental protocol provided by the manufacturer. The first step is white blood cells lysis: 25 µL of Proteinase K solution and 200 µL of Buffer NBL were added to 200 µL blood sample in a microcentrifuge tube. After mixing by vortex, the samples were incubated at 70 °C for 10-15 minutes. To remove total RNA, 10 µL of RNase (40mg/mL) were added to each sample and then incubated for 5 minutes at room temperature. In the next step, 210 µL of 100% ethanol were added to the samples and mixed immediately to obtain a homogeneous solution. The fourth step is the DNA binding to the fixed phase of the column: the mixtures are transferred to a NZYSpin Blood Column placed in a 2 mL collection tube, centrifugated for 1 minutes at 11000 xg. Then the flow-through are discarded and placed the column in a new collection tube. The DNA, bound to the silica membrane, was subjected to two series of washes, with Buffer NW1 e Buffer NW2, ethanol containing respectively. Each sample was centrifugated for 1 minutes at 11000 xg after each wash. The penultimate step requires the dried of silica membrane through a further centrifugation phase for 2 minutes at 11000 xg. The last step of the extraction allows the elution of the DNA from the NZYSpin Blood Column, that are placed in clean 1.5 mL microcentrifuge tube and are added 100 µL of elution Buffer NE directly in the membrane column, incubated for 1 minute and then

centrifugated for 2 minutes at 11000 xg. The DNA is then stored in a sterile test tube at 4 °C or 20 °C. As described previously, the concentration and purity of the DNA was determined spectrophotometrically using Nanodrop technology, by measuring respectively the absorbance at 260 nm (A 260) and the ratio between the absorbance values at 260 nm and 280 nm (A 260/280).

3.2 Primer walking

Primers used in PCR experiments were designed, for each gene, on the specific chromosomal sequences reported in the NCBI database (https://www.ncbi.nlm.nih.gov/). The accession number links to the GeneBank record (NG) of each gene is shown in table 1.

GenBank
NCBI Reference Sequence

Gene	NG number	Chromosome
PBGD	NG_008093.1	11q23
PPOX	NG_012877.2	1q22
CPOX	NG_015994.2	3q11.2
ALAD	NG_008716.1	9q34
UROS	NG_011557.2	10q26.2
UROD	NG_007122.2	1p34
FECH	NG_008175.1	18q21.3
ALAS2	NG_008983.1	Xq21.1

Table 1. *Reference sequence NG and chromosomal localization of each gene involved in the biosynthesis of heme.*

Primer pairs designed on each gene involved in the heme synthesis pathway are shown in table 2. PCR method of the coding sequence of each gene was performed using primer pairs under optimized conditions. The reaction mixes were prepared using ≈ 20 ng of purified DNA, 10x PCR Buffer B1, 5 mM $MgCl_2$ (SOLIS BIODYNE), 200 µM dNTP mix (SIGMA Aldrich), 20 picomoles of each primer (https://www.biomers.net/), 5 U/µL of HOT FIREPol DNA polymerase (SOLIS BIODYNE) in a

final volume of 25 µL.

Gene	
PBGD	
EX. 1 FOR.5'GGTGGTCGAATGGGGAGGTCCACTGTC 3'	*EX. 1 REV.5'GGAGGGCAACCGAGCTACTGGCCCTTT 3'*
EX. 2 FOR.5'CCTTATCTCTTTACCCACCTGGCTGTG 3'	*EX. 2 REV.5'GGAAGAAAGGAACTTCAGAACCTGGCC 3'*
EX. 3 FOR.5'GGCCAGGTTCTGAAGTTCCTTTCTTCC 3'	*EX. 3 REV.5'CTAACCCTCTGAGTCCCCCAATTTGTG 3'*
EX.4 FOR.5'CTTCAGGATCTGCCTAACCTGTGACAG 3'	*EX.4 REV.5'CGGGCTTTAGCTATAGGCAAAGCCAGA 3'*
EX.5 E 6 FOR.5'ATCGTAGCACAGCGCTAGGCTCAGTAA 3'	*EX.5 E 6 REV.5'GTCCCAGCAAGAGACCTAGCATACTAG 3 '*
EX.7 FOR.5'TGCTTCCTGAACTGCCCTAGGCTCCAC 3'	*EX.7 REV.5'AAGCAGAGGGTCAGGCCCCAAAGGGAA 3'*
EX.8 FOR.5'TCTGCCCTGAGGAGTGTTGACTGGTGG 3'	*EX.8 REV.5'CTGTTCCTTTCCTCCTCCTCCCATCCC 3*
EX.9 FOR.5' GCTTGGTGGGATGTGCCCAGAAGATGC 3'	*EX.9 REV.5'GACTCCCAGAGCCCTCTAGACCTTGTC 3'*
EX.10 FOR.5'AGAGGGAAAGACAGACTCAGGCAGAGG 3'	*EX.10 REV.5'TGGGGATGACTGTAAGGCAGAAAGGAG 3'*
EX.11 FOR.5'GATGATAGGGAACTCCCATCTCACTGC 3	*EX.11 REV.5'GGTCTGCCCCTCCCTGAGAATGCTATT 3 '*
EX.12 FOR.5'GCAAGTAGATAGAGGTGGTCCCATGCT 3'	*EX.12 REV.5'CCCAGACCTGGTCCTATCCATACACAA 3'*
EX.13 E 14 FOR.5'TTCAGTGATGTCCTCAGGTCTGTGGTC 3'	*EX.13 E 14 REV.5'TATGAGGGAAGGAGGTGGGATTTGGTG 3'*
EX.15 FOR.5'AAAGCTGGAGGGCGAGGGGGTAATAAA 3'	*EX.15 REV.5'GATAGCAGTGAGAATGGGGCACTGAGG 3'*

Gene	
PPOX	
EX.1 FOR. 5'GTCGCTCCGCCTCTGCCAGTTCAATGT 3'	*EX.1 REV. 5'CCCGGCCACTCACTGCTTTAGGGGAAA 3'*
EX.2 FOR. 5'GAACTCAAAACCGGCGGGGCTTCTGGA 3'	*EX.2 REV. 5'CTGACCCACCAAACATACTTCCTCCCC 3'*
EX.3 FOR. 5'GCCCTCTGAATATGCCTCTTCCCCTCC 3'	*EX.3 REV. 5'CTGACCCACCAAACATACTTCCTCCCC 3'*
EX.4 FOR. 5'GGAGGGGGCTTCCATTGGGGAATAGAG 3'	*EX.4 REV. 5'ATCCTGGGCGAGAGCGATACTCCGTCT 3'*
EX.5 FOR. 5'TGAGTGGAAATGACCCCAGCGCCTGGA 3'	*EX.5 REV. 5'GCCCCTAGGTGGTAGATTTGAACAGGG 3'*
EX.6 FOR. 5'CCCCCAACCCAAACCCTATCCCACCCT 3'	*EX.6 REV. 5'AATAGCACCCCTTGTCCCCACTCCCTC 3'*
EX.7 FOR. 5'GGCCTCCTAAAGTGCTGGGATTACAGG 3'	*EX.7 REV. 5'CCTAGGATTCTGGGGTAGCCCATGTCT 3'*
EX.8 FOR. 5'GGGAAACTGAGAGTGAGGCACCAGAAG 3'	*EX.8 REV. 5'GTCCTGCTGACCCAGGAAGGTATAGCT 3'*
EX.9 FOR. 5'CCCCTGAACTGGTCATCTCTATGGGAG 3'	*EX.9 REV. 5'TTATCTGCCCACCTCGGCCTCCCAAAA 3'*
EX.10 FOR. 5'CCCCCCAAAAAAATGGGAAGGAGAGAC 3'	*EX.10 REV. 5'ATCAGTCTGGCCTTGCCTACAATGGAG 3'*
EX.11 FOR. 5'AGTGGCATTTCCAGAGGGCTCCTCTGT 3'	*EX.11 REV. 5'CCTAGGCCTTGGCTGACATACAGTGAC 3'*
EX.12-13 FOR. 5'GAAGGCCTTGAAGACAGAGACTGGAAC 3'	*EX.12-13 REV. 5'TTCTGCATCCCAGGCACACTTTGCCTC 3'*

Gene	
CPOX	
EX.1 FOR 5'CTCCCAGCGCGCCCCAGTTCCCGCCCC 3'	*EX.1 REV 5'CCCACCAACCCCGCCAGCGCCGCGGCC 3'*
EX.2FOR. 5' GGGAAACGGGAAAATAACCATCTTCAT 3'	*EX.2 REV. 5' CGTGCGGCATATGAACCCGAATGGCTT 3'*
EX.3 FOR. 5'GCCATTCGGGTTCATATGCCGCACGTT 3'	*EX.3 REV. 5' TTTCTCGCTTTTAGATGTTATGCCCTC 3'*
EX.FOR.4 5' GCCTAGGCCTTACTGGTCTTCAGAGCT 3'	*EX.4 REV.5' GCCTCTCATTCTCAAGCATAGATGACC 3'*
EX.5 FOR. 5' GAGGATAGTGCTGTAACCTGAAAGGCT 3'	*EX.5 REV. 5' CAAAGTATCTGACAACACAACACCCGC 3'*
EX.6 FOR. 5' GATGGGAACTGGGGGGAAGAACCCACC 3'	*EX.6 REV. 5' CTCTCCTTGCCCTCATAGAGCTGTGGG 3'*
EX.7A FOR. 5'GGTACAAGGCACATCAGGCACAGTAGA 3'	*EX.7A REV. 5'GCCATCTCACCATTCATCACTGACAGC 3'*
EX.7B FOR. 5'TGCCTTAGTCTTCTCCACTCTGCACCC 3'	*EX.7B REV.5'CAGCAGAGACTTCAGTATTGACAAAGT 3'*
EX.7C FOR. 5'AATTCAGTGAAGTTGAGACTTCATAGT 3'	*EX.7C REV. 5'ATTTGCTCTTAAGAGCAAAGAGCTGCA 3'*
EX.7D FOR. 5'CACACGTTTCTTAGGAAAATGGACACA 3'	*EX.7D REV. 5'GAGTTGGGGCCCCTAGCCCTAATGTTG 3'*

Gene	
ALAD	
EX.1 FOR.5'CCCTCCAGGCCCTCGACACACCCAATT 3'	*EX.1 REV.5'GCCAGGGCTTCAGGCGCACAGCACAAT 3'*
EX.2 FOR.5'GCTAGAGAGAGGGGAGGCAGGAATCTA 3'	EX.2 REV.5'TGATGCCCGCTCCAGTCAACACTCCCT 3'
EX.3 FOR.5'TGCTTCCCAACCATCCCTCTCAGTCGC 3'	*EX.3 REV.5'CTTCTGCCTCCCAGCACTTCCACCTGT 3'*
EX.4 FOR.5'TCTAACAGAGGCACACAGTGTGGTGGG 3'	*EX.4 REV.5'GATCCACCCACTTTGGCCTCCCAAAGT 3'*
EX.5 FOR.5'GGCTATGCTCTGTGATGGCTGTCATCC 3'	*EX.5 REV.5'ATGACTGGGTTTTGGGGAGCACCTTGG 3'*
EX.6 FOR.5'ACCCACACTCCTACTGCCCACTTCTCA 3'	*EX.6 REV.5'TTCAGAACTCTGGGGCCCTCCTAGCCA 3'*
EX.7 FOR.5'AGTGAACCACCAGCAGGGATGGGCACC 3'	*EX.7 REV.5'TCTGTGATTCTTAGCAGACACGGGGGC 3'*
EX.8-9 FOR.5'TCTTTCTCTCCCTGCCACATCACCCTG 3'	*EX.8-9 REV.5'GGGATGAGGGTATAATGTGGGTGGTGC 3'*
EX.10 FOR.5'GTGAGTGACTAGGACTTGAGCCCCACC 3'	*EX.10 REV.5'GGAAGGGGAGGAGAGGATGCATGCTTA 3'*
EX.11 FOR.5'ACGGGGCTCAAGATGGTCACAGATTGA 3'	*EX.11 REV.5'TCTCAGGACGTCGTTCCCCAATCTAGG 3'*
EX.12 FOR.5'CACAGGCTGTGCTTCTTCATGGTAGCC 3'	*EX.12 REV.5'GCAGGAAGAGGGCATGAGGGCACAGTT 3'*
Gene	
UROS	
EX.2 FOR 5'GTGTACCGTCCCCATCGGAAATTGCTT 3'	*EX.2 REV 5'TTTTGCAAAACCCATCCCTGCCTGCTC 3'*
EX.3 FOR 5'GAGCAGGCAGGGATGGGTTTTGCAAAA 3'	*EX.3 REV 5'AAATAGTCCCTCTCTGGCTTCAGCTGG 3'*
EX.4 FOR 5'ACTCAGTAAGTGTTGGGGGGATGGGTG 3'	*EX.4 REV 5'GCAGCTGCTTCTGGAATTTAGTCTCCC 3'*
EX.5 FOR 5'TGAACAAGCAGCCTTGGGCAACAGTCC 3'	*EX.5 REV 5'GCATACATACTGACCAAGTGGTTCTCA 3'*
EX.6 FOR 5'GAACAGACACTTGTGATCTTCCCTCAG 3'	*EX.6 REV 5'CTTTTCCCTAGGTAGTGGTTGTGAGGT 3'*
EX.7 FOR 5'GCTTCCCCCTTCCCAAAGCTGCCCCTC 3'	*EX.7 REV 5'TTGTGTGCTCTCTGCAGGGCCACCCAC 3'*
EX.8 FOR 5'AACTGTGCTGTGAAGTGGTGGAGGCCC 3'	*EX.8 REV 5'ATCTATCAGCTCGTGCCCTTCACCCTC 3'*
EX.9 FOR 5'ATGCGGATGAAGCCGGAGGAATGTTGT 3'	*EX.9 REV 5'GGGTGTCTCACTTGACATTGAAGCCCT 3'*
EX.10 FOR 5'GCCCCTGCACACATCCAGCTGCCTGCT 3'	*EX.10 REV 5'GGGTTATCAGAGGTGGGCATACCTGTC 3'*
Gene	
UROD	
EX.1 FOR.5'GCCTTTGTTGTTGCGTCGCTACAGCAA 3'	*EX.1 REV.5'AAAGGGGAGTAGAGGGATAGAGTCCTG 3'*
EX.2 FOR.5'AGTTTGTGCACCACCTGATAGGCAGAG 3'	*EX.2 REV.5'TACAGAGGGAAGACAGGGCTCAGCCTT 3'*
EX.3-4 FOR.5'ACTCCGGAGGGAGAAAAGTTTTCGAGG 3'	*EX.3-4 REV.5'TTCCCTCGATCCAGTTAGGATAAGTGC 3'*
EX.5 FOR.5'CCTCCTGGAATGAGCTGAACAGAACCT 3'	*EX.5 REV.5'ACCCTTCCTTTTGTCTACCCCAGACCT 3'*
EX.6 FOR.5'TCACTCTGGAAGGTCTGGGGTAGACAA 3'	*EX.6 REV.5'CTGCCCTCTCAGGTTTAGGACACTCTT 3'*
EX.7 FOR.5'GGGTCAGGCAGTATCAGGGATTGAAGT 3'	*EX.7 REV.5'TGGTCACTCCAGTCCATGCAGGACTTA 3'*
EX.8-9 FOR.5'TGGAGGGCAGCAGAAGTACAGTCAGA 3'	*EX.8-9 REV.5'AGTCCGGTCTTTCTAGGGCTTATGTTG 3'*
EX.10 FOR.5'CTGAGTAGAAGCATGCCTACATATGCG 3'	*EX.10 REV.5'CCCTACCCCATGTAGTTCTGGGACTTA 3'*
Gene	
FECH	
EX.1 FOR. 5'CCCATTTTCACGCAGGGAGCGGCGCCC 3'	*EX.1 REV. 5'CAGCACCCCCAAGGCCGCTCCCCGAAT 3'*
EX. 2 FOR. 5'CCCCTTGGAGAGGGCTTAAGTTCCTTT 3'	*EX.2 REV. 5'TTTTCCCAGCACCTTTCCTCCCAGGCA 3'*
EX 3 FOR. 5'TTGCTGGCTGAACCAAGAGTCCACCCT 3'	*EX.3 REV. 5'CCCACTAACTTATTTGCTCTCTCCCCC 3'*
EX.4 FOR. 5'CTGGGTATTCCTCAGAGAGGGTATAGC 3'	*EX.4 REV. 5'GCCAGTACATATGAAGCATTTAGCATC 3'*
EX. 5 FOR. 5'ACTTGCCTTCACCGTCAGTGCCATAGG 3'	*EX.5 REV. 5'CATCCTTCCCTTCAGTACTTAGACTCC 3'*
EX.6 FOR. 5'TGATTCAGTAAAGAAGCAGTTACCTGC 3'	*EX.6 REV. 5'CACAAACCCAGAAGGGATGAGAAGCTG 3'*
EX.7 FOR. 5'CCCTAGGCCCCTGAAACTGTTATGATC 3'	*EX.7 REV. 5'GCTTAGGACATAATGGAAGCTGGACCC 3'*
EX.8 FOR. 5'TGTGTCAGCACATAGTCAGAGGCTCTC 3'	*EX.8 REV.5'CCCCTTCTATCTTACTCGCTTGCAGAG 3'*
EX.9 FOR. 5'AGCAGGTGTAAAGAGTGGCTCTTGCCC 3'	*EX.9 REV.5'TCAGGAGAATGAGGACACCGTACATGC 3'*
EX.10 FOR. 5'GAGCAGTCTGCGAACAGTTGAAGTCAG 3'	*EX.10 REV. 5'GGTGGGTAGAAATCAGAAAATTGGGGC 3'*
EX.11 FOR. 5'TTTGGTTCAAAGGGCTCACCACTCGGA 3'	*EX.11 REV. 5'ACACCCTCTCCACATCGGAGGTATCTG 3'*

Table 2. *Primer pairs (https://www.biomers.net/) designed on each gene involved in the heme pathway.*

3.3 Agarose gel electrophoresis

The DNA fragments obtained by PCR were separated by 2% agorose gel electrophoresis in 1X TBE, using known molecular weight markers. Agarose gel were prepared using 1.2 g of agarose (EuroClone), 60 mL of TBE 1X (EURx) and 2 µL of intercalant and heating in a microwave. 6 µL of PCR product was collected in new tubes and added 4 µL of 5X Orange G loading dye, for a final volume of 10 µL. The electrophoretic runs were carried out at 120 V constant in TBE 1X, in an electrophoretic chamber, for 30 minutes. The PCR fragments were visualized by UV transilluminator and compared with the molecular weight markers used.

3.4 DNA purification

PCR products were purified using GeneMatrix PCR/DNA Clean-up Purificatione kit (EURx). The kit is equipped with spin-columns and various buffers that removed primers, nucleotides, enzymes, mineral oils, salts and other impurities present in the DNA samples. 30 µL of activation buffer DX were applied onto the centre of the spin-column to permit the membrane activation and kept it at room temperature. Two volumes of orange-coloured Orange DX buffer were added to one volume of the DNA samples and mixed.

The mixture was transferred onto the DNA binding spin-columns and centrifuged at 11000 rpm for 1 minute, then the supernatants were poured off and placed back into the receiver tubes. DNA samples were subjected to two series of washes, respectively with 500 µL of buffer Wash DX1 and 600 µL of Wash DX2 and, after centrifugation, the spin-columns were placed into new collection tubes. 100 µL of elution buffer (heated to 80 °C), were added to elute bound DNA, incubated for 1 minute at room temperature and spun down for 1 minute at 11000 rpm. Isolated DNA was stored at 2-8 °C until sequencing reactions.

3.5 Sanger Sequencing

Purified fragments were sent in liquid phase added with respective reverse and forward primers to Bio-Fab Research srl (Rome) and to Hospital Universitario 12 de Octubre (Madrid, Spain) for Sanger sequencing. The chromatograms for each fragment were analysed by Chromas 2.4 software. The sequences, reconstructed by assembling the individual sequenced PCR fragments, were aligned each other using Nucleotide Blast, and then compared using Human Blast (http://blast.ncbi.nlm.nih.gov/Blast.cgi) with the respective reference sequences for each step of the sequencing.

4 Results

This study was carried out to 1 Italian patient from Sardinia (including living family members, i.e. mother and sister), and 53 patients from Spain (some unrelated and others for family studies). Each patient read and signed informed consent.

The sequence analysis, conducted on the CPOX and FECH gene of Italian patient affected by VP, have highlighted some polymorphisms not directly associated with the patient phenotype. Five polymorphisms were found in CPOX gene: c.557-51 A>C in exon 2, c.810-131 C>T in exon 4 and c.12989+1 A>G c.13171+53 G>T c.13171+66 G>C in exon 5. In FECH gene were found nine polymorphisms c.18492+23 A>G in exon 3, c.28864+37 A>T c.28864+38 T>G in exon 6, c.32585+1C>G in exon 7, c.36893+94T>A in exon 8, c.37321+1A>G in exon 9 and c.40423+30G>A c.40423+56G>A c.40423+92G>A in exon 10.

As shown in table 3, the sequence alignment of the Italian patient compared with those of the database, showed the presence of numerous heterozygosis in the intron zones flanking the coding exons, subject to alternative splicing events, and different SNPs in the exon regions which however do not involve amino acid changes. Mutations in the areas flanking the coding sequences can

compromise the correct formation of the spliceosome. In fact, the formation of the spliceosome involves a complex interaction of many factors that include small particles of nuclear ribonucleoproteins (snRNP, U1, U2, U4 / U6 and U5), small nuclear RNAs (snRNA) and associated proteins as well as ~150 additional proteins. The binding of snRNPs to pre-mRNA is stabilized by mutual interactions between introns and exons[57].

Furthermore, as shown in figure 13, an insertion of six nucleotides 18505_6insTATTCT was found in the 3' UTR region of the CPOX gene, which is an important region for the half-life of the messenger. Genetic variants in 3 'UTR are also implicated in disease susceptibility due to the change in RNA structure and protein translation.

Gene	***Polymorphism***	***Location***
FECH	c.18492+23 A>G	Exon 3
	c.28864+37 A>T c.28864+38 T>G	Exon 6
	c.32585+1C>G	Exon 7
	c.36893+94T>A	Exon 8
	c.37321+1A>G	Exon 9
	c.40423+30G>A c.40423+56G>A c.40423+92G>A	Exon 10
CPOX	c.557-51 A>C	Exon 2
	c.810-131 C>T	Exon 4
	c.12989+1 A>G c.13171+53 G>T c.13171+66 G>C	Exon 5
	18505_6insTATTCT	Exon 7

Table 3. *Polymorphisms found in FECH and CPOX gene in the Italian patient.*

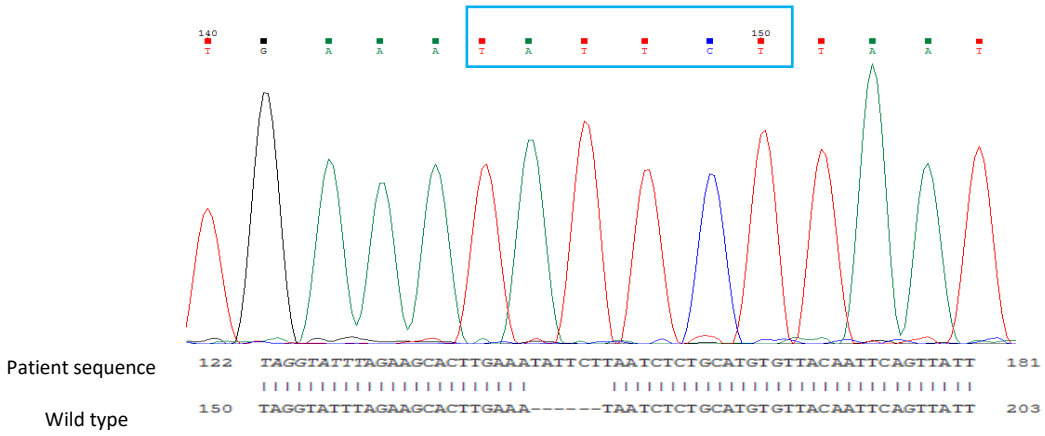

***Figure 13**. Chromatogram shown the Insertion 18505_6insTATTCT found in exon 7 of 6 nucleotides in 3'UTR of CPOX gene.*

PPOX chromatograms shown the presence of an insertion of an A nucleotide, four nucleotides upstream to the exon 3, and variety insertions in coding region of exon 3. Frameshift mutations c.5710_5711ins.CG, c.5714_5715ins.A, c.5720_5720ins.CT, which cause a shift in DNA reading compared to the normal sequence present in NCBI database, were found on exons 3 in PPOX gene. The same analysis was repeated twice on both patient and healthy subjects (under the same analysis conditions), in order to verify the presence of these frameshift mutations.

The chromatograms confirm the presence of new frameshift mutations in the Italian patient, which is compatible with VP. The sequencing of exon 3 highlighted numerous heterozygosity in the whole coding region, difficult to analyse due to the different insertions found.

The patient's phenotype, according to clinical analysis, is associated with mutations in the PPOX gene.

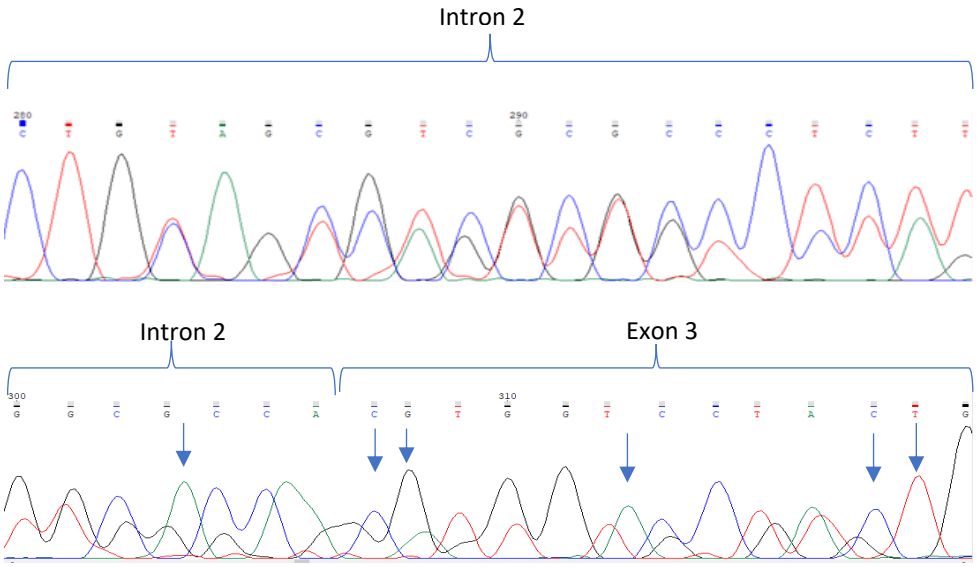

Figure 14. *Chromatograms of intron 2 and the first part of exon 3.The arrows show nucleotides in heterozygosis and diverse nucleotide Insertions, one in intron 2 IVS.2-4ins.A and five in exon 3: c.5710_5711ins.CG, c.5714_5715ins.A, c.5720_5720ins.CT*

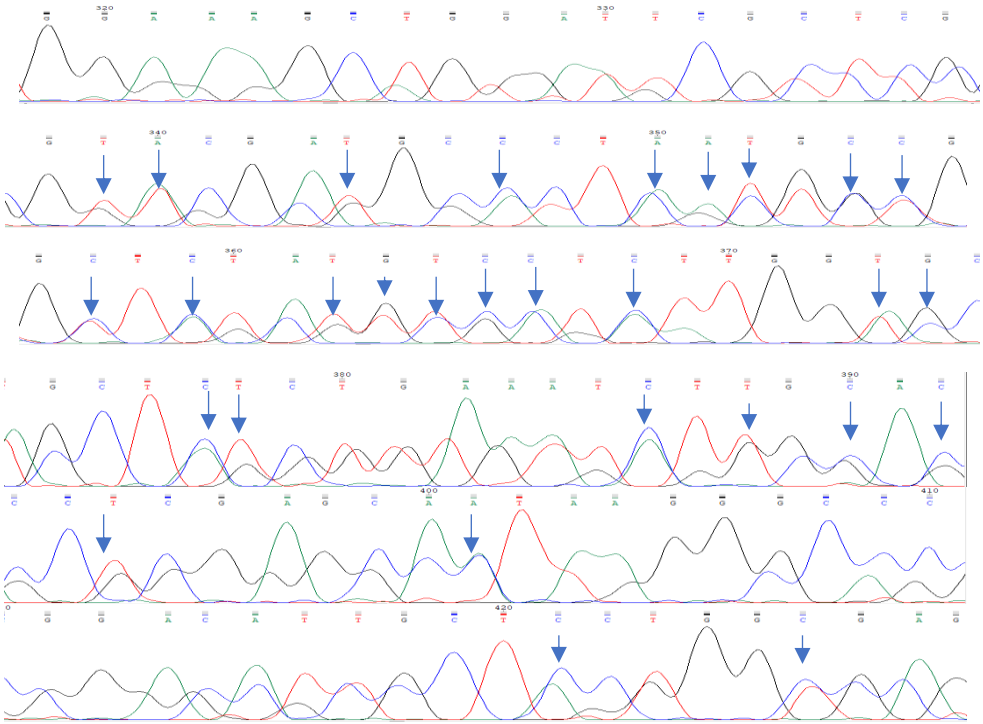

Figure 15. *Chromatogram of exon 3 of PPOX gene, shows diverse heterozygosis.*

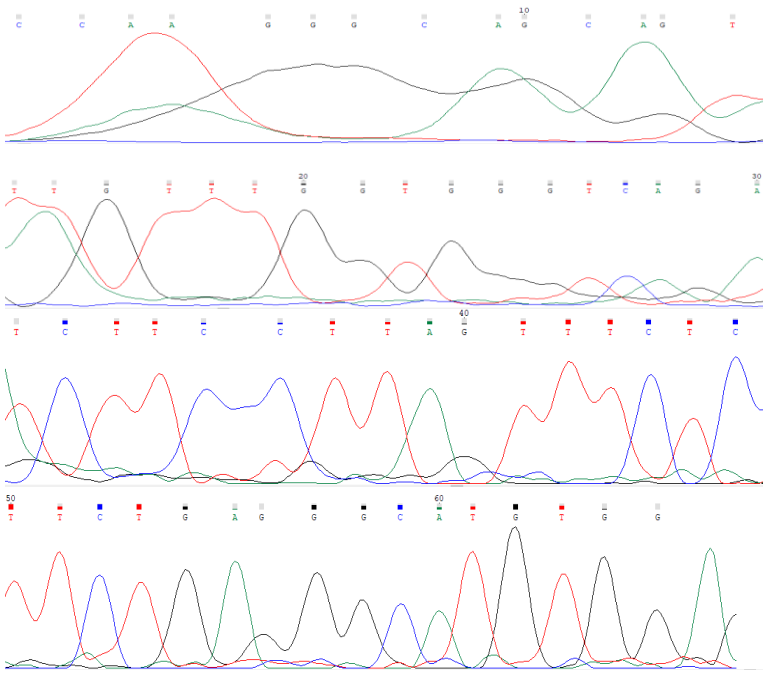

```
Query  12  AGT-TGTTTGGTGGGTCAGATCTT-CCTTAGTTTCTCCTCTTCTGAGGGCATGTGG  65
           ||| ||||||||||||||||||| ||||||||||||||||||||||||||||||
Sbjct  40  AGTATGTTTGGTGGGTCAGATCTTCCCTTAGTTTCTCCTCTTCTGAGGGCATGTGG  95
```

Figure 16a. *Chromatogram of exon 4 of PPOX gene (query),*
shows the premature stop of lecture compared with wild-type named as (Sbjct)

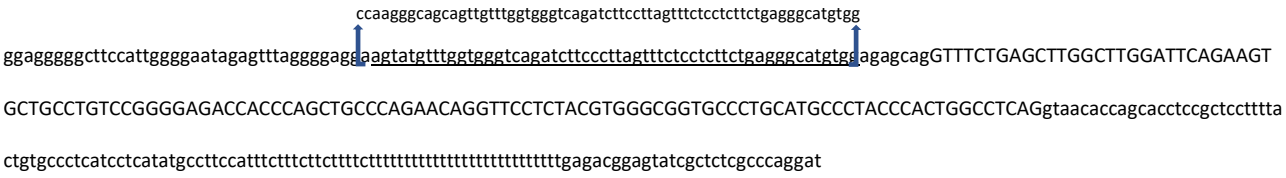

Figure 16b. *Wild-type sequence of exon 4 of PPOX gene. The intronic sequences are in lowercase letters, while the wild-type coding exonic sequence in capital letters. Above, as shown in this figure, the sequence of the patient compared, using blast tools, which finds complementarity only in the intronic zone, presumably due to the frameshifts present in exon 3.*

As shown in table 4, genetic studies of related and unrelated patients affected by various types of porphyrias, were performed using biological samples of the Spanish population. The patients were analyzed in the Hospital Universitario 12 de Octubre (Madrid, Spain), in the Center for rare and genetic diseases (porphyrias, hemochromatosis and anemia group). The study was performed on 53 patients aged between 14 and 77, of which 37 were women. The clinical manifestations of these patients were helpful in an initial diagnosis: some patients had acute symptoms, others manifested skin photosensitivity, while some patients had both symptoms. Genetic analysis was performed, after isolating the DNA from leukocytes cells. The results shown in the table 4 highlight mutations already described in Spanish population, while in the case of family studies, patients confirm the same mutations found in probands. Two unrelated individuals showed the founding mutation 669_698del of PBG gene. The founder effect is a special case of genetic drift, which occurs when a small group of a population separates from the original population and forms a new one. The new population may have less genetic variation than the original population and, through the randomization of alleles during reproduction of subsequent generations, rapidly continue towards fixation[58]. The identification of this mutation allowed a quick and simple molecular diagnosis of AIP in families in Spain, particularly those belonging to the Murcia region[59].

Some new mutations have been found in patients with AIP: one affected consensus splice sites Ivs11+3A>T in intron 11 which resulted in aberrant splicing. The other one was an insertion which caused a frameshift mutation c.41_42ins.A in exon 3 of PBGD gene that led to a change in the reading frame with the introduction of a premature stop codon.

PBGD gene mutations		
Patient, Sex, Age	***Mutation***	***Location***
P1, F, 16	Ivs11+3A>T	Intron 11
P2, F, 22	c.-150T>A	Exon 1
P3, F, 50	Ivs4-3C/G	Intron 4
P4, M, 48	c.669_698del.30	Exon 12
P5, F, 56	c.340_341ins.T	Exon 7
P6, F, 63	c.874ins.C	Exon 14
P7, F, 59	c.340_341ins.T	Exon 7
P8, F, 42	Ivs4+4A>G	Intron 4
P9, F, 32	c.973C>T	Exon 15
P10, M, 53	Ivs12+3_+11del.AGGGCCTG	Intron 12
P11, F, 54	c.-150T>A	Exon 1
P12, F, 69	c.973C>T	Exon 15
P13, F, 45	c.748_749insCATCGCTG	Exon 12
P14, F, 51	Q34P	Exon 6
P15, F, 19	Ivs4+4A>G	Intron 4
P16, M, 15	Ivs4+4A>G	Intron 4
P17, M, 49	c.107_110del.ACAG	Exon 4
P18, M, 14	c.107_110del.ACAG	Exon 4
P19, F, 40	c.340_341ins.T	Exon 7
P20, F, 55	c.-150T>A	Exon 1
P21, F, 37	c.669_698del.30	Exon 12
P22, F, 69	c.340_341ins.T	Exon 7
P23, M, 77	c.340_341ins.T	Exon 7
P24, F, 34	M212V	Exon 11
P25, F, 59	M212V	Exon 11
P26, M, 31	c.340_341ins.T	Exon 7
P27, F, 26	c.655G>C	Exon 10
P28, M, 74	c.340_341ins.T	Exon 7
P29, F, 45	c.340_341ins.T	Exon 7
P30, F, 59	Ivs.4-3C>G	Intron 4
P31, F, 46	c.41_42ins.A	Exon 3

PPOX gene mutations		
Patient, Sex, Age	***Mutation***	***Location***
P32, F, 43	p.R168H	Exon 6
P33, F, 60	c.451C>T	Exon 5
P34, F, 58	c.451C>T	Exon 5
P35, F, 62	c.451C>T	Exon 5
P36, F, 30	p.Q151X	Exon 5
P37, F, 72	p.R168H	Exon 6
P38, F, 59	c.503G>A	Exon 6
P39, F, 52	c.503G>A	Exon 6
P40, M, 50	p.R168H	Exon 6
P41, F, 53	p.R168H	Exon 6

UROD gene mutations		
Patient, Sex, Age	***Mutation***	***Location***
P42, F, 34	p.G281E	Exon 4
P43, M, 52	p.L253Q	Exon 6
P44, M, 71	p.G281E	Exon 4
P45, M, 63	983del.TT	Exon 8

CPOX gene mutations		
Patient, Sex, Age	***Mutation***	***Location***
P46, F, 58	c.341_342del.GG	Exon7
P47, M, 37	c.1102del.C	Exon 5
P48, F, 74	c.1102del.C	Exon 5
P49, M, 40	c.32del.G	Exon 1
P50, M, 39	c.1102del.C	Exon 5
P51, F, 19	p.L82P	Exon 3

FECH gene mutations		
Patient, Sex, Age	***Mutation***	***Location***
P52, M, 71	c.599-1006_c.1078-1135del. 11478bp	Exon 3
P53, F, 64	Ivs.1as-23C>T, Ivs.3as4T>C	Intron 1, Intron 3

Table 4. *Results obtained from genetic studies of related and unrelated patients, with various types of porphyrias in Spaniard patients at Hospital 12 de Octubre (Madrid, Spain), Center for rare and genetic diseases. Porphyrias, hemochromatosis and anemia group.*

5 Discussion

The sequencing results obtained from the analysis of the chromatograms performed on the Italian patient allowed the detection and characterization of numerous polymorphisms in CPOX and FECH genes, the sixth and last enzyme in the heme pathway, respectively associated with HCP and EPP. The five polymorphisms found in CPOX gene (c.557-51 A>C in exon 2, c.810-131 C>T in exon 4 and c.12989+1 A>G c.13171+53 G>T c.13171+66 G>C in exon 5), and the nine found in FECH gene (c.18492+23 A>G in exon 3, c.28864+37 A>T c.28864+38 T>G in exon 6, c.32585+1C>G in exon 7, c.36893+94T>A in exon 8, c.37321+1A>G in exon 9 and c.40423+30G>A c.40423+56G>A c.40423+92G>A in exon 10) did not involve any amino acid substitutions that did not cause a change in the amino acid sequence of the protein concerned. This type of silent mutations is mainly neutral since they do not compromise the functionality of the protein encoded within which the mutated triplet is found. The numerous heterozygosis present in both CPOX and FECH genes were close to the donor consensus junction sites between the exons and the introns and therefore, could affect splicing.

The new insertion of 6 nucleotides 18505_6insTATTCT found in the seventh exon of the CPOX gene, is located in the 3'-untranslated region, the noncoding part of mRNAs. 3'-UTRs play an important role in the biology of higher organisms because they regulate the destiny of mRNA, including degradation, translation and localization[60]. Moreover, 3'-UTRs are involved in the fate of proteins through the regulation of protein-protein interactions, are also able to form protein complexes with various compositions[60]. The possible role of 3'-UTRs in the pathophysiology of diseases and mutations affecting function is not yet well known. The available data suggest that this region, often underestimated during genetic screening of genes associated with diseases, may plays an important part in various diseases and in their progression. Indeed, mutations affecting the termination codon, the polyadenylation signal or the secondary structure of the 3'-UTRs may cause de-regulation and disease. For example, alterations in the length of the 3'-UTRs may alters the position of the physiological termination codon and consequently affect the translation of mRNA[61]. For all these reasons, the insertion found in the 3'-UTRs of exon 7 of the CPOX gene may play an important role in the messenger half-life and these variants are often involved in metabolic dysfunctions and disease pathogenesis.

Chromatogram analysis of the PPOX gene were performed on the Italian patient. The coding sequence in this gene starts in exon 2. Results showed numerous heterozygosis starting from 26 nucleotides upstream of exon 3, precisely in the intronic flanking region. In proximity of the coding sequence, four nucleotides upstream of exon 3, an insertion of an A has been found in intron 2 (IVS.2-4ins.A). This region, which is located in proximity to the coding sequence, is subject to alternative splicing events. If mutations in introns or exons occur at the splice sites, can be incurred a loss of site functionality which can cause: a premature stop codon on the exon, inclusion of an intron in mature RNA, displacement of the splice site with consequent insertion or deletion of some

amino acids, transposition of the splice site which involves inclusion of less or greater number of bases and therefore the resulting exons will be shorter or longer[62].

Frameshift mutations found were additions or deletions disturbing the reading frame, so that the entire set of codons downstream of the mutations were impaired in reading[63]. In exon 3 were found new frameshift mutations: c.5710_5711ins.CG, c.5714_5715ins.A, c.5720_5721ins.CT, as shown in figure 16a and 16b, which lead on a stop signal in exon 4. A stop codon (or termination codon) is a triplet of nucleotides located within the messenger RNA that signals the end of the translation process of the current protein. Frameshift mutations in DNA can cause hidden premature stop codons. The polypeptide created could be abnormally short or long or will not be functional. Hidden stops are non-stop codons that terminate translation prematurely due to a shift in ribosomal RNA. Out-of-frame stops are shifted by -1 and +1 and are hypothesized to decrease resource waste on non-functional proteins and the production of potential cytotoxins[64].

Figure 15 shows the exon 3 sequencing chromatogram, in which numerous heterozygosis are highlighted for the entire coding region. Due to the different insertions found, it was not possible a correct reading of the DNA respect to the wild-type present in NCBI (NCBI Reference Sequence: NG_012877.2). In fact, the insertion of one or more bases leads to the sliding of all the triplets from the insertion point onwards. This implies that in translation, the triplet interpretation mechanism, which initiates the reading at the level of the first AUG codon on the mRNA and continues to read the next three bases, will be profoundly altered by the moment a triplet that including the base inserted is not present in the normal sequence. The position of the normal bases is found shifted forward and the error affects the reading of all subsequent triplets. In this case, the frameshift mutation phenomenon involves adding the wrong amino acids from the mutation point onwards, resulting in the formation of a premature stop codon in the next exon. In any case, the natural sequence of amino acids is severely altered.

Based on the patient's clinical and phenotypic manifestations, we might speculate that the mutations, found in exon 3 of the PPOX gene, lead to VP. In fact, the patient presents symptoms such as skin lesions in the parts of the body exposed to the sun and damage to the oral mucosa and teeth, as typical of this type of porphyria, that reinforced our hypothesis.

Results obtained (table 4), were performed at Hospital Universitario 12 de Octubre (Madrid, Spain), during my abroad period at the Center for rare and genetic diseases, in the porphyrias, hemochromatosis and anemia group. This study was carried out on related and unrelated patients, with various types of porphyrias. Genetic studies conducted on relatives of probands affected by porphyria confirm the mutations already found in the probands, validating the familiarity of the disease.

Here we report a 669_698del mutation of the HMBS gene in two individuals from independent Spanish AIP families. All carriers of this mutation share a disease-associated haplotype indicating an ancestral founder effect. Unfortunately, the story behind the founding effect of this mutation in Spain is not well known, but the region of Murcia, a southeastern region of Spain, is identified as the geographic location from which this mutation started[65].

Two new mutations have been found in patients with AIP: Ivs11+3A>T in intron 11 and c.41_42ins.A in exon 3 (figure 17).

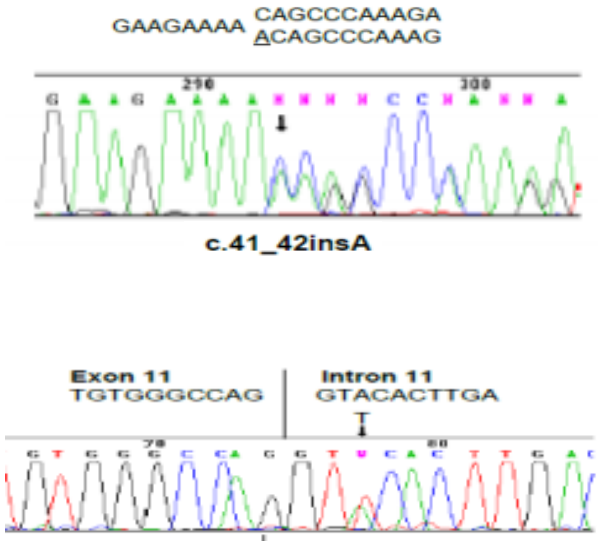

Figure 17. *Mutations found in patients with AIP: c.41_42ins.A in exon 3 and Ivs11+3A>T in intron 11.*

The novel intronic mutation, that affect consensus splice sites, was c.651 + 3A>T in the donor site of intron 11 (IVS11+ 3A > T) and caused an aberrant splicing. The mutation consisted of an A to T transversion at the donor site (position c.651 + 3). In this case, RT-PCR studies have shown that the mutation results in the preservation of the entire 240 nucleotides of intron 11 in the mature transcript. The insertion c.41_42insA located in exon, consisted of a single adenine insertion between positions c.38 and c.41. This mutation caused a frameshift in the reading frame and introduced a stop signal of translation at codon 52, in exon 4.

These results emphasize the molecular heterogeneity of the AIP in Spain. This study also allowed a correct diagnosis in asymptomatic heterozygotes family members. The identification of asymptomatic heterozygotes is important in order to contain the occurrence of neurovisceral attacks that are dangerous for patients with porphyrias. Through large-scale molecular studies it will be possible to know the prevalence of AIP in Spain. Therefore, the identification of a founding mutation is of greatest importance for AIP screening strategies among Spaniards of southern ancestral origin.

Genetic analysis is the most reliable and accurate methodology to confirm the diagnosis and especially for the identification of latent carriers.

PART 2:

BIOCHEMICAL ANALYSIS OF PORPHYRIN INTERMEDIATES IN BIOLOGICAL FLUIDS

1 Porphyrin precursors determination in human urine

Urine is important for understanding kidney and systemic disease. It is an easy to obtain body fluid and can be analysed in different ways for different diagnostic and therapeutic pathways[66]**.**

In this disease, urine are valid diagnostic indicators to discriminate various types of porphyrias. In fact, during neurovisceral crises caused by acute porphyrias, porphyrin precursors such as delta-aminolaevulinic acid and porphobilinogen are mostly eliminated in urine[67] (compared to healthy individuals from <2 mg/L to over 110 mg/L)[68].

An essential tool for diagnosing porphyria attacks is the Hoesch's test. The Hoesch's test allows for a quick and easy assessment of urinary PBG. Positive results require quantitative urinary PBG determinations to confirm suspected porphyria[69]. The test consists of 1 mL of Ehrlich's reagent (2 g dimethylaminobenzaldehyde in 20% hydrochloric acid) to which 2-3 drops are added from a fresh patient urine sample, protected from light. If the Ehrlich's reagent, in contact with urine, assumed pink intense or red colour the test is considered positive, otherwise it is negative.[70] The colour is intensified by exposure to light (figure 18).

2 Porphyrin precursors determination in human blood

Diagnostic blood tests performed in symptomatic patients suspected of porphyria are based on the determination of plasma erythrocytes and porphyrins[71]. A preliminary test for the diagnosis of differentiation from symptomatic porphyrias is the fluorescent assay of plasma porphyrin with a characteristic peak at 618–620 nm[71]. In whole blood, plasma and erythrocytes, increasing amount of protoporphyrin IX can be detected and quantified, as a diagnostic indicator[72], using the Piomelli's method[73].

MATERIALS AND METHODS

3 Chromatographic-spectrophotometric determination of total porphyrins and separation of uro-porphyrins and copro-porphyrins in urine

24-hour urine protected from light was collected from patients with positive Hoesch test for suspected acute porphyria. 0.5 mL of urine and 4.5 mL of 37% HCl were transferred into a 10 mL tube and, after a short vortex, the absorbances of the samples were measured using a fluorimeter. Samples with an absorbance > 200 nm were analysed by column chromatography.

The kit produced by FAR srl, with an accurate protocol, was used for the determination of total porphyrins and the separation of uro and copro porphyrins in the urine. Porphyrins were adsorbed in two chromatographic columns each containing anionic resin. After measuring the volume of the collected urine, an aliquot was taken to which sodium carbonate was added to obtain a 1% (w/v) solution. Samples were stored overnight at room temperature, protected from light. Samples are stable for one week. Total porphyrins were obtained bring urine to 5.0 pH value with glacial acetic acid and incubate in a boiling water bath for 30 minutes. 1 mL of urine was added both in column 1 and in column 2 (supplied in the kit) for total porphyrins and uro-porphyrins respectively. When the liquid of mobile phase was completely flow, 5 mL of distilled water and 5 mL of acetate buffer were added (twice). The eluate was discarded, and the columns were placed over clean test-tubes, then 2.5 mL of 2X hydrochloric acid were added. After vortexing, the absorbances of the eluates were read on the spectrophotometer and the differences between the absorbances values (ΔA) obtained for the total porphyrins and the uro and copro-porphyrins were calculated according to the following Allan's formula:

$$\Delta A = 2A\ (400\text{-}407\ nm) - [\ A\ (380\ nm) + A\ (480\ nm)\ ]$$

3.1 Chromatographic-spectrophotometric determination of 5-Aminolevulinic acid (ALA)/ porphobilinogen (PBGD)

ALA and PBGD precursors were quantified using a specific kit (BioSystem S.A.), following the protocol provided by the manufacturer. The samples were passed consecutively through two chromatographic columns that contain ionic exchange resins: a column retains porphobilinogen while the other one retains 5-aminolevulinic acid. A PBGD microcolumn containing a pre-weighted amount of a buffered anionic exchange resin and an ALA microcolumn containing a pre-weighted amount of a buffered cationic exchange resin, were taken for each urine sample. Each PBGD column was placed on top of the ALA column and, one at a time, 10 mL of distilled water, 1 mL of urine and 20 mL of distilled water were pipetted into the PBGD. The eluates passed through the column were discarded. PBGD columns were separated from ALA columns and stored in the dark in order to quantify PBGD later. Fresh tubes were placed below ALA columns and 10 mL of 1 mol/L sodium acetate were pipetted, collected the eluate to which was added 0.2 mL of acetylacetone. A blank sample containing 0.2 mL of acetylacetone and 10 mL of sodium acetate, and a standard sample containing 9.9 mL of sodium acetate and 0.2 mL of acetylacetone and 0.1 mL of standard ALA were prepared. Each sample was incubated in a boiling water bath for 10 minutes. After boiling water bath, 1 mL of Ehrlich's reagent was added to the samples, to the blank sample and to the standard (PBGD samples must turn pink). Later all samples were incubated, protected from light, for 15 minutes at room temperature. ALA and PBGD were spectrophotometrically quantified by the absorbance at 555 nm of the Ehrlich's reaction product.

3.2 Quantification of protoporphyrin IX in whole blood (Piomelli's method)

The protoporphyrin in erythrocytes is accumulate in red blood cells when iron is not present in sufficient amount in the synthesis of heme. A small percentage of protoporphyrin can be measured as free erythrocyte protoporphyrin, while remaining protoporphyrin (approximately 90%) is measured as zinc protoporphyrin.

The first test for suspected porphyria in the blood is the plasma fluorometric assay. Plasma was separated from whole blood and 1 mL of saline buffer was added to 0.5 mL of plasma. Positive samples were analyzed using a fluorometer and the data obtained were compared with negative control data. On the basis of the observed peak, we proceed with the quantification of protoporphyrin IX following the protocol.

The analysis was done in the dark condition. In a tube, 100 µL of plasma was added with 300 µL of PBS (Phosphate Buffered Saline), in another tube 100 µL of whole blood was added with 300 µL of PBS. Then, 2 mL of ethyl acetate /acetic acid 4:1 (v/v) has been added to each sample, which were vortexed and centrifuged for 5 minutes at 1500 rpm. After centrifugation, the supernatant was recovered and was transferred into a graduated crystal tube. Subsequently, was followed a step in which 2 mL of HCl was added to each processed sample, which were vortexed and centrifuged for 1 minute at 2000 rpm with the purpose to separate the phases. The volumes of the hydrochloric phase (lower phase) were noted, and the absorbance was read in the fluorimeter compared to the blank sample with the following parameters:

λ excitation at 405nm

λ emission at 595nm

emission peaks between 619-621 nm are peculiar to HCP, CEP and AIP. Emission peaks between

634-636 nm instead is typical of EPP while emission peaks between 626-628nm is typical of VP.

3.3 PBGD enzymatic activity in erythrocytes

PBGD enzymatic activity was performed on blood samples previously stored at -80 °C. 500 µL of red blood cells were aliquoted and dilutes 1: 3. 200 µL of hemolysis buffer was added to 100 µL of red blood cells and mixed. Hemolysis was performed subjecting the samples to 3 repeated freeze-thaw cycles: 3 minutes at -80 °C and then 1 minute at 37 °C. After that, hemoglobin was quantified by dilution of the lysate 1: 3 made using 20 µL of red blood cell lysate which was added to 40 µL of PBS. Hemoglobin standard curve was made using 150 mg/mL of a powdered human hemoglobin preparation (SIGMA). Dilutions were prepared with 50 mg/mL hemoglobin and 0.1 M TRIS-HCl incubation buffer; pH 8. 1 mL of Drabkin's reagent was added to 8 µL of lysate (dilution 1: 3) and left for 10 minutes at room temperature. The absorbance was read at 540 nm. 200 µL of incubation buffer was added to 25 µL of lysate diluted to the necessary hemoglobin concentration. A pre-incubation of 5 minutes was performed at 37 °C. Then, a phase of incubation at 37 °C in the dark condition was carried out for 1 hour. Following, 1 mL of 10% trichloroacetic-acid (TCA), was added to the samples, which have been vortexed, placed on ice for 10 minutes and then exposed to light for 20 minutes to activate the oxidation of porphyrins. Finally, the samples were centrifuged for 10 minutes at 10000 rpm. The supernatant obtained was collected and analyzed in the fluorimeter with the following setting:

λ excitation at 405 nm

λ emission at 595 nm

3.5 Quantitative determination of porphyrins in faeces

The determination of porphyrins and their precursors in faeces is of fundamental importance in establishing the diagnosis of porphyrias. The quantification of coproporphyrin and protoporphyrin in faeces occurs following a protocol divided into steps. The first step concerns the calculation of the dry weight: the fecal samples of porphyrin patients of porphyria were weighed. After weighing an empty glass tube, 3 g of stool was weighed, and the total weight noted.

The sample was placed in an oven at 80 °C for 24 hours. Samples were weighed every 24 hours for 5 days. In the second step, the samples were prepared to be processing: an empty glass tube was weighed, and 0.5 g of faeces was added, and then the total weight was noted.

The tubes were filled with ethyl ether with the aim to wash the samples which were centrifuged for 3 minutes at 1500 rpm. Next, the samples were loaded into a decanter tube and placed in a transilluminator at 360 nm to check for fluorescence and then to confirm the positivity.

The washes were repeated three times until samples stopped being fluorescent. After washings, 5 mL of sodium acetate at 3%, 1-2 drops of iodized solution were added to a decanter tube. After mixing the solutions, 2 phases are formed: the lower phase was discarded, and this step was repeated two more times. 5 mL of distilled water was added, mixed, eliminated the gases and eliminated the lower phase. In the third stage, coproporphyrin is extracted. 5 mL of 0.1% HCl were added to the sample, mixed and the lower phase was collected in a graduated tube containing coproporphyrin. Washes with HCl were repeated until the lower phase was no longer pink. In the fourth step, protoporphyrin is extracted. 5 mL of 5% HCl were added, mixed and the lower phase was collected in a graduated tube containing protoporphyrin. Washes with HCl were repeated until the lower phase was no longer pink.

The samples were then analyzed on the spectrophotometer to measure the absorbance and calculated following the formula provided by the manufacturer:

2xDmax- (Abs 430+ Abs 380) x E x final volume (mL) x F/ initial weight of faeces in g

D max= Abs at 402 nm (coproporphyrins) + Abs at 409 nm (protoporphyrins);

E = molar extinction coefficient (0.730 coproporphyrins, 1.226 protoporphyrins);

F= (total weight- weight of empty tubes)/ (dry weight- weight of empty tubes)

4 Results

Thirty unrelated individuals of Spanish origin, aged between 14 and 77 years of whom 23 were women, were studied biochemically. All patients were diagnosed and were followed up clinically at the Hospital Universitario 12 de Octubre. If preliminary biochemical laboratory results support acute porphyria, eg. elevated urinary PBGs or porphyrins, or skin lesions caused by cutaneous porphyria due to elevated plasma or urinary porphyrin levels, additional biochemical diagnostic tests are needed to differentiate acute and cutaneous porphyrias and conditions associated at liver disease that cause nonspecific porphyrinuria.

Diagnosis of AIP was based on clinical symptoms, increased excretion of ALA and PBG in urine and faeces such as as well as reduced erythrocyte HMBS activity. Of these patients, some were in remission at the time of the study, others treated prophylactically with hematin (3-4 mg / kg every 8-10 days). These patients had previously experienced more than 30 acute attacks, while other patients had suffered between 1 and 7 attacks.

An essential tool for diagnosing porphyria attacks is the Hoesch’s test. This test allows a quick and easy evaluation of urinary PBG. The test consists of a preparation containing 1 mL of Ehrlich's reagent (2 g dimethylaminobenzaldehyde in 20% hydrochloric acid) to which two drops of fresh urine were added. After gentle shaking, the reagent changes color to a reddish tone, confirming the

positivity of the acute porphyria attack (figure 18). If the reagent does not change color, the test is negative and excludes that abdominal pain is due to a porphyritic crisis in progress[67].

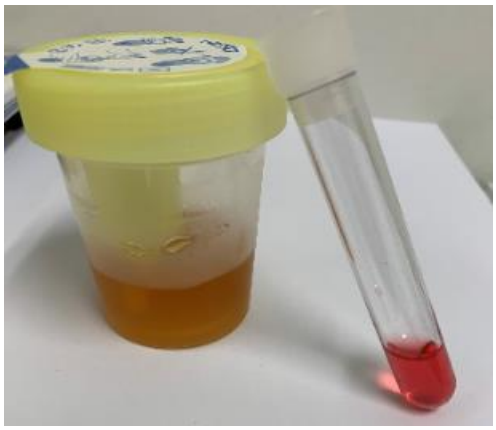

Figure 18. *Example of a positive Hoesch's test.*

The urine sample of the positive patients was subjected to further biochemical investigations to quantify and determine the porphyrin precursors.

Urine and fecal samples showed elevated levels of porphyrin products compared with normal values. Normal urinary values for ALA are ≤ 7.5 mg / L, while urinary PBG in healthy subjects is ≤ 2.5 mg / L. The correct values for urinary porphyrins are instead ≤ 200 µg / g of creatinine and for fecal porphyrins are ≤ 30 µg / g dry weight. Few patients had values close to the reference values provided by the protocols, most of them showing a quantity of strongly altered porphyrin intermediates in both urine and faeces. Fecal porphyrins were analyzed in ten patients aged 26 to 77, of which eight were women. In this analysis were quantified coproporphyrins and protoporphyrins, typical intermediates found in patients' faeces with porphyrias.

Patients with acute and photosensitive symptoms, having a prevalence of fecal coproporphyrin, characterized by classical plasma fluorescence scan emission peak between 619 and 621 nm, were

also genetically analyzed at the level of the CPOX gene which was sequenced to confirm HCP. Patients only with acute symptoms, characterized by plasma fluorescence scan peaked at 626-628 nm and elevated fecal protoporphyrins, underwent to genetic analysis, through the sequencing of PPOX gene, to confirm the VP.

The activity of HMBS was calculated in 20 AIP patients (table 5). Patients shown reduced enzymatic activity, especially in those patients with frequent acute attacks, in which these data were also accompanied by marked increases in ALA / PBG concentrations. However, some patients may have normal erythrocyte HMBS activity even during a crisis with acute attacks. This depends on several factors including hormonal factors that play an important role in stabilizing the levels of porphyrin intermediate in the blood. Enzymatic assay may play a decisive role in the AIP diagnosis[74].

The uroporphyrinogen I, spontaneously produced by PBGD conversion, was oxidized by exposure to light and then fluorometrically quantified.

The plasma of the patients was preliminarily placed on the transilluminator set at 360 nm to verify the fluorescence indicating the positivity of the sample. The quantification of protoporphyrin IX was measured using the Piomelli' s method[73] (table 6). The analysis was conducted on six patients, with various porphyrias, of both sexes and aged between 16 and 52 years. Patients, who showed the typical emission peak, were analyzed to detect the amount of protoporphyrin IX. A negative result does not imply that the patient does not have porphyria. Plasma fluorescence scanning is a more reliable test than, for example, fecal porphyrin analysis, especially as regards the diagnosis of VP. Patients with VP have a characteristic maximum fluorescence emission peak at an excitation wavelength of 626 ± 1 nm which allows patients with VP to be identified from those with other porphyrias[75].

Sensitivity and specificity of these tests were higher in adults than in children / adolescents and higher in adults with disease symptoms than in asymptomatic carriers[75].

QUANTIFICATION OF URINE AND FECAL PORPHYRINS				
PATIENT, SEX, AGE	**URINE ALA (mg/L) n.r. ≤ 7.5**	**URINE PBGD n.r. ≤ 2.5**	**TOTAL PORPHYRINS (µg/g Creatinine) n.r. ≤ 200**	**HMBS ACTIVITY %**
P1, F, 46	13	21	435	48
P2, F, 32	38	146	1226	78
P3, F, 45	31	31	524	65
P4, F, 22	9	10	364	69
P5, F, 16	126	143	527	59
P6, M, 48	28	66	127	49
P7, F, 50	12	32	253	68
P8, F, 56	10	5	205	71
P9, F, 63	20	25	2210	54
P10, F, 59	20	23	2264	53
P11, F, 42	87	235	127	49
P12, M, 53	9	5	911	65
P13, F, 54	125	109	794	64
P14, F, 69	55	103	1115	55
P15, F, 51	21	28	801	48
P16, F, 19	19	68	11258	55
P17, M, 15	127	143	527	59
P18, M, 49	37	62	887	74
P19, M, 14	12	32	246	68
P20, F, 40	43	89	992	50
PATIENT, SEX, AGE	**URINE ALA (mg/L) n.r. ≤ 7.5**	**URINE PBGD n.r. ≤ 2.5**	**TOTAL PORPHYRINS (µg/g Creatinine) n.r. ≤ 200**	**FECAL PORPHYRINS ≤ 30 µg/g dry weight**
P21, F, 55	8.4	3.5	428	932
P22, F, 37	8.6	3.9	280	109
P23, F, 69	11	4	1297	618
P24, M, 77	8	2	448	128
P25, F, 34	13	4.3	288	1492
P26, F, 59	7	4	280	118
P27, F, 26	15.2	14	1124	230
P28, M, 74	9.8	2.8	2103	1020
P29, F, 59	36	39	1724	425
P30, F, 46	60	46	1164	581

Table 5. *Quantification of urine and fecal porphyrins. Normal values: Urine ALA: ≤ 7.5 mg/L; Urine PBG: ≤ 2.5 mg/L; Urine Porphyrins: ≤ 200 µg/g creatinine; Fecal Porphyrins: ≤ 30 µg/g dry weight. HMBS: erythrocyte hydroxymethylbilane synthase activity expressed as the percentage of the fluorescence intensity.*

QUANTIFICATION OF PROTOPORPHYRIN IX IN WHOLE BLOOD (PIOMELLI'S METHOD)			
PATIENT, SEX, AGE	PLASMA SCAN	WHOLE BLOOD	PLASMA
P1, F, 32	627,23 nm	34,61 µg/dL	3,267 µg/dL
P2, F, 23	620,75 nm	33,88 µg/dL	34,69 µg/dL
P3, M, 40	621,65 nm	4,644 µg/dL	27,702 µg/dL
P4, F, 16	618,19 nm	3,834 µg/dL	33,723 µg/dL
P5, M, 39	619,77 nm	10,53 µg/dL	37,206 µg/dL
P6, F, 52	633,13 nm	11,87 µg/dL	34,235 µg/dL

Table 6. *Quantification of protoporphyrin IX in whole blood (Piomelli's method). Normal values: Plasma scan: negative (no emission peak). Whole Blood: 22,10±12,87µg/dL; Plasma: 0,93±0,32 µg/dL.*

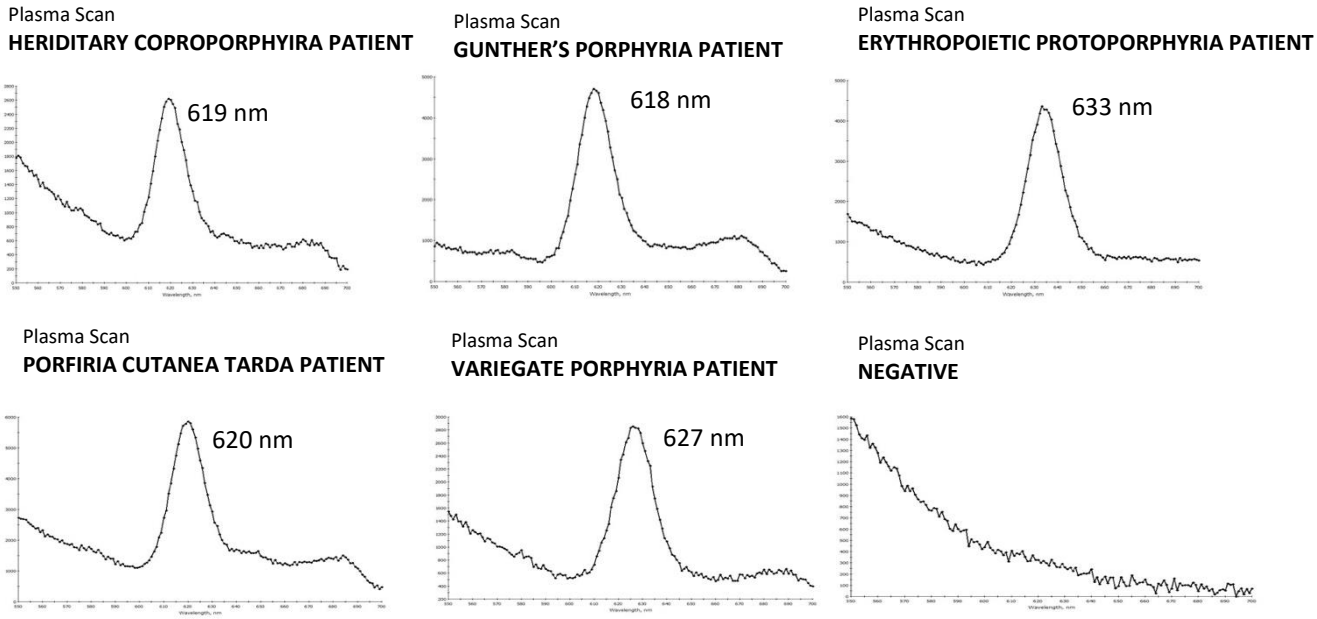

Figure 19. *Fluorescence emission spectra recorded using plasma samples: Peaks between 619-621 nm are peculiar to Coproporphyria, Gunther's Porphyria and Acute intermittent porphyria, between 634-636 nm is typical of Protoporphyria, while the peak between 626-628 nm is of the Variegate Porphyria. Normal values: Plasma scan: negative (no emission peak).*

5 Discussion

Four different types of acute porphyrias are known: AIP, VP, HCP and ALADP. These porphyrias have some common symptoms due to the accumulation of ALA and PBG which cause neurovisceral attacks. During acute attacks, urinary excretion of precursors PBG and ALA increase significantly.

In this study, the patients showed some altered levels compared to the reference values of urinary ALA and PBG in healthy subjects. In the thirty patients analyzed, ALA values in urine varied between 7 and 127 mg / L, but normal values are ≤ 7.5 mg / L. PBGD values in urine showed a range between 2 and 235 mg / L compared to ≤ 2.5 which correspond to normal reference values. There are also alterations in the total porphyrins present in the urine of these subjects, in which the values obtained vary between 127 and 11258 mg / L compared to ≤ 200 mg / L in the normal range. Therefore, these data demonstrate that acute attacks were caused by acute porphyria.

For screening, it is important to measure also total porphyrins in the same urine sample, as PBG

levels may be less elevated in VP and HCP than in AIP and decrease to normal levels more rapidly. Although a substantial increase in PBG indicates disease, an increase in urinary porphyrins do not indicate porphyria, because urinary porphyrins are increased in many other clinical conditions, especially when the hepatobiliary system or bone marrow is affected.

In patients in remission, values of PBG and total porphyrins may not increase. In this case, if acute porphyria is suspected to have caused past symptoms, comprehensive biochemical tests including urinary ALA, fecal porphyrins, and plasma porphyrins should be performed[14].

The excessive PBG concentration in urine is identified by performing the Hoesch's test[67]. The Hoesch's test was performed on patients who manifested acute attacks with abdominal pain. The samples tested positive, then required quantitative determinations to confirm the suspected porphyria, such as the quantitative determination of porphyrin precursors in the urine, in the faeces and in the blood as demonstration that the acute attack was really attributable to an acute attack of porphyria.

Plasma fluorescence scanning is a sensitive test that is used for porphyrin analysis[75]. The reading of the emission peaks of the plasma samples fluorescence scan, is important to understand the type of patient's related porphyria. The absorbance and fluorescence scans were done in fused quartz cuvettes with a path length of 1 cm. Emission peaks between 619-621 nm are peculiar to HCP, CEP and AIP. Emission peaks between 634-636 nm are instead typical of EPP, while emission peaks between 626-628 nm are typical of VP. Figure 19 shows the most significant plasma fluorescence scan values in patients affected by: HCP (scan emission at 619 nm), CEP (scan emission at 618 nm), EPP (scan emission at 633 nm), PCT (scan emission at 620 nm), VP (scan emission at 627 nm) and a negative profile with no emission peak. The fluorescence of the samples is given by a mixture of porphyrins which include uroporphyrin, harderoporphyrin, isoharderoporphyrin, protoporphyrin and pentacarboxylic porphyrin[75]. These analytical data are important to carried out further specific

genetic and biochemical analysis to confirm the results.

AIP, in addition to the characteristic clinical symptoms, is diagnosed by the presence of elevated levels of urinary porphyrin precursors such as ALA and PBG as well as reduced erythrocytic activity of HMBS[74]. As shown in table 5, the enzymatic activity of HMBS was calculated, through the use of the fluorimeter, in 20 AIP patients aged between 14 and 69 years of both sexes, ranging between 48-78 %. The fluorimeter was set up with λ excitation at 405 nm and λ emission at 595 nm. HMBS activity is expressed as the percentage of the fluorescence intensity. The more HMBS activity values approach 100 %, the more the enzymatic activity is normal, in fact low values indicate pathogenicity. It is a qualitative and not a quantitative analysis, in fact brothers' patients with the same mutation show different enzymatic activity. This evidence is related to hormones. In fact, female hormones often may change and stabilize the activity of the enzyme. Both CPO and PPO are allosteric inhibitors of HMBS, consequently its activity is impaired[25]. The diagnostic measurement of erythrocytic HMBS activity has limits, as demonstrated in some studies, the results could be influenced by several factors that may affect both the condition of the erythrocytes and the state of health of the patient. For example, an increase of the reticulocytes in the circulation is known to interest enzyme activity by increasing the values. It is therefore not surprising to find erythrocytic HMBS activity normal during acute attacks and decreased compared to normal during remissions[74].

Analysis of fecal porphyrins, analyzed in ten patients, showed that coproporphyrin and protoporphyrin levels increase during an acute attack. Fecal porphyrins are particularly high in HCP and VP, while in AIP the increase is minimal. The reference value ≤ 30 µg / g dry weight of the profirins present in the faeces is considered as an optimal diagnostic threshold. All patients analyzed show remarkable levels of copro and proto porphyrins with values ranging from 118 to 1492 µg /g dry weight, considerably exceeding the threshold considered normal. The fecal porphyrin pattern allows the differentiation between HCP and VP, in fact in HCP there is a marked predominance of

coproporphyrin III and approximately equal increases of coproporphyrin III and protoporphyrin in VP[75].

The biochemical analysis carried out during my abroad period in Madrid, demonstrate to be in line with the genetic analysis performed on patients suffering from different types of porphyria. Molecular studies were carried out to confirm the clinical diagnosis, especially when the biochemical studies were not complete, and also to detect asymptomatic gene carriers in the family. The results presented in this work demonstrate that molecular techniques represent the most accurate approach to identify latent carriers. These studies are very important especially in prepubertal children where neither fecal nor plasma porphyrins allow the identification of the carrier status of some types of porphyrias such as VP[14].

PART 3:

PROTEOMICS INVESTIGATION OF THE ACID-SOLUBLE FRACTION OF SALIVA FROM PORPHYRINIC PATIENTS

1 Human saliva in proteomic research in detection and characterization of potential biomarkers

The term proteomics was coined by Marc Wilkins in 1996 to indicate the protein complement of the genome. Proteomics is a science that deals with the qualitative and quantitative study of total proteins expressed by a cell, an organism or a tissue. Proteomics is useful for other sciences such as transcriptomics and genomics, to comprehend structures, functions and interactions of proteins[76]. Proteins play a crucial role in sustaining life, as the multiple functions of specific cells are regulated by many different types of specialized proteins. Furthermore, post-translational modifications (PTMs), such as sulfation, phosphorylation, hydroxylation, methylation, glycosylation, occurs in eukaryotic cells at different sites by numerous ways creating a microheterogeneity.

Since proteins can change their expression in response to different stimuli, proteomics-based technologies are important for studying the proteome[77]. Proteomes can be studied by various proteomic platforms: top-down or bottom-up platforms which depend principally on mass spectrometry analysis. The top-down strategy is based on protein detection without any proteolytic cleavage and offers information on PTM proteins, but sample preparation for mass spectrometry analysis requires acidification and consequently precipitation of some proteins. In addition, some proteins are difficult to detect, especially in case of high molecular weight and glycosylated ones. The bottom-up approach, on the other hand, is based on the identification of proteins and on the characterization of their amino acid sequence by digesting the proteins enzymatically or chemically. The bottom-up requests a pre-purification step such as electrophoresis or liquid chromatography. The disadvantage of this strategy is that some protein fragments are too small to be detected and as a result, information on PTMs can be lost[78].

Proteomics is a valid investigation tool in the search for biomarkers in specific pathologies, as it allows the study of many proteins and peptides present in the organism such as tissues, plasma, urine, saliva, synovial liquid and cerebrospinal fluid[79].

Human saliva is a body fluid useful for diagnosing diseases since the collection is safe and easy and has the advantage of being considered a non-invasive process for patients. Saliva can be used as a diagnostic tool for discovery of biomarkers, because pathological stages are reflected not only in the oral cavity but also on the whole organism[80].

In patients with cutaneous porphyria, skin lesions caused by porphyrin precursors that are activated by exposure to the sun in parts of the body such as the face, also affect the oral cavity, creating serious lesions to the oral mucosa. As mentioned above, the accumulation of these precursors may also cause a brownish discoloration in the teeth. The salivary study of these patients aims to identify specific biomarkers for the diagnosis of this disease, using a bottom-up approach based on SDS-PAGE used for the separation of the proteins, followed by in-gel trypsin digestion, and characterization by high-resolution mass-spectrometry.

Human saliva is composed by specific salivary proteins secreted by the three couples of major glands and non-secretory proteins that originated from the cells of the oral mucosa, from the oral flora and from the crevicular gingival fluid. Secretory proteins include: proline-rich proteins PRPs (acidic, basic and glycosylated), α-amylase, carbonic anhydrase, immunoglobulins (IgA and IgG), salivary mucins (MUC5B and MUC7), type II cystatins (S, SA, SN, C and D), histatins, statherins and P-B peptide; while non-secretory proteins include: thymosins, defensins, type I cystatins (A and B), S100 (A7, A8, A9, A11, A12) proteins, polymeric immunoglobulin receptor and antileukoproteinase[81].

1.1 Proline-rich proteins (PRPs)

PRPs represent the most preponderant of salivary proteins due to the high number of variants and post-translational modifications. They are divided into three types: acidic (aPRPs), basic (bPRPs) and glycosylated (gPRPs)[82].The proteins are coded by a cluster of six genes, strictly associated in a segment of ∼4.0 Kb in length on chromosome 12 at band 13.2.

1.1.1 Acid PRPs (aPRPs)

Secreted mostly by parotid gland, aPRPs are divided into 5 categories: PIF-s, Db-s, Pa codified by PRH1 gene and PRP1 and PRP2 codified by PRH2. Their name is due to the presence of acidic amino acid residues of aspartate and glutamate in the N-terminus. In the N-terminal region of all acidic PRP isoforms, there is a pyroglutamic acid residue and two phosphorylation sites in Ser_8 and Ser_{22} [83]. These two phosphoserine residues are essential in their role in mineral homeostasis. aPRPs are cleaved post-translationally after Arg_{106} (Arg_{127} in Db-s) by a convertase generating PRP3, PRP4, PIF-f, Db-f and the PC peptide of the C-terminal fragment. The Pa protein, which is the exception, has a cysteine residue instead of an arginine at position 103, thus resisting the activity of convertase[84].

1.1.2 Basic (bPRPS) and Glycosilated PRPs (gPRPs)

Secreted by parotid glands, bPRPs are encoded by the genes PRB1, PRB2, PRB3, PRB4 and PBII (SMR3B). PRB1 and PRB3 consist of four alleles: small (S), medium (M), large (L) and very large (VL), while PRB2 and PRB4 have S, M and L alleles. The bPRP, expressed as pre-proproteins, after the removal of the signal peptide are cleaved before the glandular secretion, generating peptide II-2 from alleles S, M and L, peptides PE and protein IB-6 from allele S, protein Ps -1 from the M allele and Ps-2 protein from the L allele allele. From the L allele of PRB2, peptides IB-1, P-J, P-H, P-F and the protein IB-8a derive, causing a single nucleotide polymorphism $Ser_{100} \rightarrow$ Pro[85]. The PRB3 and PRB4 genes encode glycosylated proteins. The M allele of PRB3 encodes the PRP3-M protein and N- an O-glycosylation sites have recently been identified[86]. The PRB4 gene encodes the PRP4 protein cleaved by an endoprotease into three chains: protein N1, glycosylated protein A and PD peptide. Glycosylation is important as it confers lubricating properties similar to the other high molecular weight proteins present in saliva, useful in the protective action of the oral cavity against abrasion and helps speech[87]. The gPRPs have different properties, for example they are able to interact with

the tannins of the diet giving a lower perception of astringency[88]. Moreover, they bind oral bacteria, such as *Fusobactrium nucleatum* present in the oral cavity in the first years of life [89]. In fact, they are the only PRPs expressed early in children, possibly acting as a first line of defense against bacterial infections in the mouth[90].

1.2 α-amylase

Secreted by both parotid and minor salivary glands, α-amylase represent one of the main salivary components and are characterized by the high number of PTMs. About 25% of α-amylase is found as a glycosylated form[91]. The main function of α-amylase is expressed during digestion, as it hydrolyzes (1→4)-alpha-D-glucoside bonds in polysaccharides such as starch. These proteins have a short time of active contact with starch in the mouth, in fact once the food bolus has been ingested, the salivary α-amylase is promptly inactivated by the gastric pH[92]. The coding genes is located on chromosome 1p21.1.

1.3 Carbonic Anhydrase 6 (CAVI)

Secreted by the parotid and submandibular glands, CAVI is an isoenzyme encoded by the CA6 gene, (located on chromosome 1), that catalyzes the $CO_2 + H_2O \rightleftharpoons HCO3^- + H^+$ reaction[93]. It has been shown that this isoform plays a protective role towards the enamel pellicle by converting (as shown in the reverse reaction) salivary bicarbonate and hydrogen ions supplied by microbes into carbon dioxide and water. However, the role of CAVI is not entirely clear[94].

1.4 Immunoglobulins (Igs)

Encoded by the genes located on chromosomes 14q32.33, 2p11.2 and 22q11.2, immunoglobulins (Ig) are antigen recognition molecules, consisting of two identical heavy chains and two identical

light chains named kappa or lambda in which, by disulfide bonds, bind a heavy chain to a light chain and the two heavy chains together. In the heavy and light chains there is a variable N-terminal region which acts as the binding site of the antigen and a constant C-terminal region which acts as a signal[95]. The Ig perform a defense function against the antigens both in the mucous layer due to the secretory IgA, and in the enamel acquired on the tooth due to the IgG predominant in the saliva. Secretory IgA, stimulated by antigens that target the mucosa, derives from local plasma cells (PCs) of the salivary glands and mucous membranes. Secretory IgA are present in dimeric form and, in some cases, in polymeric form[96]. Salivary IgG derives from serum and, through the gingival fissures, passes into the saliva. IgG is found in monomeric form. In human saliva other Igs such as IgM, IgD and IgE are also found in small quantities[97].

1.5 Mucins

Secreted by the submandibular glands, mucins are highly glycosylated proteins. In the oral cavity, the most common forms are: secreted MUC5B, MUC7, MUC19 and associated with the membrane MUC1 and MUC4. In saliva the most present are MUC5B and MUC7, which are able to bind both salivary proteins with antimicrobial properties, increasing their concentration in the oral cavity, and various bacterial strains through residues of sialic acid or proteins expressed on the bacterial surface[98]. The coding genes are located on human chromosome 11p15 and 7q22.

1.6 Cystatins

Cystatins are a family of proteins divided into types: type 1, which are encoded by the CSTA and CSTB genes and include cystatin A and cystatin B also called stefins; type 2 which include cystatin C, D, E, F, S, SN and SA expressed by a family of genes (localization: 3q21.1); type 3 comprising low and

high molecular weight kininogen and single chain glycoproteins with multiple disulfide bonds named T-kininogens. The main function of cystatins is to inhibit the cysteine proteases present in saliva[99]. Type 1, of intracellular origin, are expressed in various cells and tissues. They are inhibitors of cathepsin L, S and H. Structurally they consist in single chain proteins (about 11 kDa) with a N-terminal acetylation but without signal peptide. Type 2 are extracellular proteins (about 13-14 kDa) that include five S-types (S, S1, S2, SA and SN) and cystatins C and D and present the signal peptide[99]. Cystatin C is a single-chain protein composed by four conserved cysteine residues that can form two disulfide bridges[99]. Cystatin D exists, due to a gene polymorphism, in two natural forms which include Cys or Arg at position 26 of the chain and disulfide bridges[100]. Cystatin S is the only phosphorylated on Ser1 (S1) or on Ser1 and Ser3 (S2)[101].

1.7 Histatins

Secreted by the parotid and submandibular glands, histatins are low molecular weight peptides encoded by the HIS1 and HIS2 genes located on chromosome 4q13[102 103]. Histatin 1 is phosphorylated in Ser2 in the consensus sequence Ser_2-Asp_3-Glu_4 and partially sulphated on the last four Tyr residues (Tyr 27, 30, 34 and 36)[104]. Histatin 3 has a substitution of Glu_4 with Ala_4, hindering the phosphorylation of Ser_2. This histidine rich peptide is cleaved before being secreted, forming fragments and Histatin 5 and 6[105]. Histatins present a domain of residues that confer antifungal and antibacterial functions, especially in histatins 3, because histatin 1 does not have these characteristics but is involved in the interaction with the minerals of the tooth enamel[106].

1.8 Statherin and P-B peptide

Secreted by the parotid and submandibular glands, staterins are tyrosine-rich phospho-peptides encoded by the STATH gene located on chromosome 4q13.3. Statherins are found in the di-phosphorylated forms on Ser2 and Ser3, mono-phosphorylated and non-phosphorylated form. The presence of an intra molecular bridge that can be formed between Lys_6 and Gln_{37} through the enzymatic activity of a type 2 transglutaminase, it gives the statherins the ability to assume a cycle structure[107]. One of the properties of these proteins is to create an enamel film on the teeth, in particular cyclo-staterin, and to prevent the precipitation of calcium phosphate, due to some acid residues present in the first six N-terminal amino acids: two phosphoserine, aspartic acid and glutamic acid residues[108].

Secreted by parotid, submandibular and sublingual glands, P-B peptide is encoded by PROL3 gene located on chromosome 4q13.3, in linkage to the statherin gene, suggesting a probable functional correlation with this protein. The statherin role is known, while the functions of P-B peptide is still unclear[109].

1.9 α-defensins

Present in the gingival crevicular fluid, α-defensins are encoded by the genes (located on chromosome 8) DEFA 1, DEFA3 and DEFA4 in α-defensin 1, 3 and 4 respectively, while α-defensin 2 arises from the proteolytic cleavage of the N-terminal portion of α-defensin 1 or 3[110]. These are basic peptides rich in tyrosine and cysteine residues and play different roles such as: antimicrobial activities, cytokine production, inhibition of natural killer cells, tumor suppressor and regulation of cell volume[111].

1.10 β-thymosins

Originating from the gingival crevicular fluid, β-thymosines are encoded by two genes: TMSB4X gene (clustered on chromosome Xp22.2), which expresses oxidized thymosines β4 (Tβ4) and β4 and TMSB10 gene (located on chromosome 2p11.2), which expresses thymosin β10 (Tβ10)[112].

They have multiple important functions, including actin polymerization, bone marrow stem cell proliferation, metalloproteinase induction, angiogenesis, inflammation inhibition, and chemotaxis[113].

1.11 S100 family

The S100 family is divided into three subfamilies: S100A (A7, A8, A9, A11, A12), S100B and S100P encoded by genes located on chromosome 1q21. These proteins have the characteristic of being able to modulate the functions of other proteins when they bind calcium ions. In fact, they participate in both intra and extracellular functions including calcium homeostasis, cell growth and differentiation, protection from microbial activity, contraction and motility, transport of arachidonic acid, chemotaxis, cytoskeleton rearrangement, apoptosis, control of ROS formation, inflammation and protein phosphorylation and secretion[114].

1.12 Antileukoproteinase

Antileukoproteinases have a complex origin, in fact they are produced by different cells such as neutrophils, macrophages, β cells, epithelial cells of the renal tubules, acinar cells of the parotid and submandibular glands but also by acinar and epithelial cells. They are expressed by the SLPI gene, located on chromosome 20q12-13.2. Their role includes the inhibition of protease, trypsin, elastase, and chymotrypsin, chymase and tryptase[115].

1.13 Polymeric Immunoglobulin Receptor (pIgR)

The submandibular and parotid glands express the polymeric immunoglobulin receptor (pIgR) gene which is located on chromosome 1q31-q41. PIgrs are type 1 transmembrane glycoproteins and play a role in mucosal immunity as they are capable of carrying polymeric IgA through mucosal epithelial cells. pIgRs are subject to a proteolytic cleavage that occurs in the glycosylated extracellular region, releasing the secretory component called SC which is important in functions related to the oral mucosa[116].

2 The oral manifestations of porphyrias

Cutaneous or non-acute porphyrias, can be distinguished into four types: CEP, PCT, EPP and XLP. These porphyrias showed an accumulation of porphyrins in the skin and in the liver with consequent photosensitivity and possible liver damage [7]. Skin lesions, accompanied by blistering, mainly affect the sun-exposed areas, especially of the hands and face.

Porphyrins accumulation is reflected in different areas of the body and among these also in the oral mucosa, where bubbles and erosive lesions can develop at muco-buccal and palate level[17].

In a study published in 2000, a patient aged over 60 was described with PCT and Hodking's lymphoma, that manifested cutaneous lesions on the lower lip. The patient presented with ulcers and oedema and difficulty in speech and eating due to bleeding blisters[117].

In CEP patients a common symptom is the deposition of red-brown pigments in the bones and teeth known as erythrodontia[118]. Erythrodontia is caused by the accumulation of porphyrin precursors which appear as a discoloration of the dentition, especially in the dentin and in the enamel due to the affinity of porphyrins for calcium phosphate[119].

MATERIALS AND METHODS

3 Sample collection, treatment and subjects enrolled

Whole saliva (from 0.5 to 1.0 mL) was collected from 23 adult patients from Spain divided in 3 groups per type of porphyria and 23 adult age/sex matched healthy subjects with a soft plastic aspirator. Samples were collected between 8,30 and 13.00 a.m. in fasting patients. Immediately after collection, each sample were mixed in 1:1 ratio in a solution with 0.2% 2,2,2 trifluoroacetic acid (v/v; TFA) containing Leu-enkephalin (Leu-Enk 50uM) as internal standard and transferred in a plastic tube and then in an ice bath. The samples were then centrifuged at 14000 rpm for 10 min at 4°C, and the acid soluble and insoluble fractions obtained were separated and stored at -80°C until the analysis.

3.1 SDS Page

The three pools of patients and the pool of controls were analysed by SDS-page in reducing and non-reducing using the condition previously indicated. The analysis was carried out using a gel that was stained with Bio-Safe TM Coomassie G250 stain (Bio-Rad, Hercules, CA, USA) to be submitted to an in-gel tryptic digestion.

3.2 In-gel tryptic digestion

The SDS-PAGE gel obtained in reducing and non-reducing conditions were submitted to an extensive excision along every line. Stained protein bands and the lines that did not show stained, were manually excised from the gel and transferred to fresh tubes. The gel pieces were washed with 100 mM ammonium bicarbonate, then with 100 mM ammonium bicarbonate/50% acetonitrile v/v (ACN, Sigma-Merck, St. Louis, MO, USA) and finally with ACN (10 minutes each wash) to de-stain the

gel pieces. The protein's cysteine residues were reduced with 10 mM dithiothreitol for 30 minutes at 65°C, in the dark and alkylated with 55 mM iodoacetamide for 30 min at RT, in the dark. The gel pieces were washed first with 100 mM ammonium bicarbonate and then with ACN, dried and rehydrated in digestion buffer (40 mM ammonium bicarbonate/ultrapure ACN in 10:1 v/v ratio) containing high-specific trypsin (Trypsin Single, Proteomics grade – Sigma-Merck, St. Louis, MO, USA), with a ratio of 1:30 (w/w) of enzyme to substrate. The samples were incubated overnight at 37°C. After the incubation, 0,1% of formic acid (FA) was used to block the reaction. Extraction of tryptic peptides was performed by two-fold addition of 100 mM ammonium bicarbonate/ACN in 1:2 v/v ratio. Tryptic peptides were lyophilized and stored at -80°C until the analysis.

4 Results

After quantifying proteins present in each saliva sample, 3 separate saliva pools were created for patients with porphyria and 1 saliva pool from healthy subjects with the same sex-age ratio as patients. All pools were prepared with a final concentration of 0.41 g / µL. The first pool includes 12 patients with AIP, the second pool of 4 patients with VP, the third pool instead includes 4 patients with HCP. Finally, the control group includes 20 healthy individuals. As shown in figure 20, each pool was loaded twice in the gel.

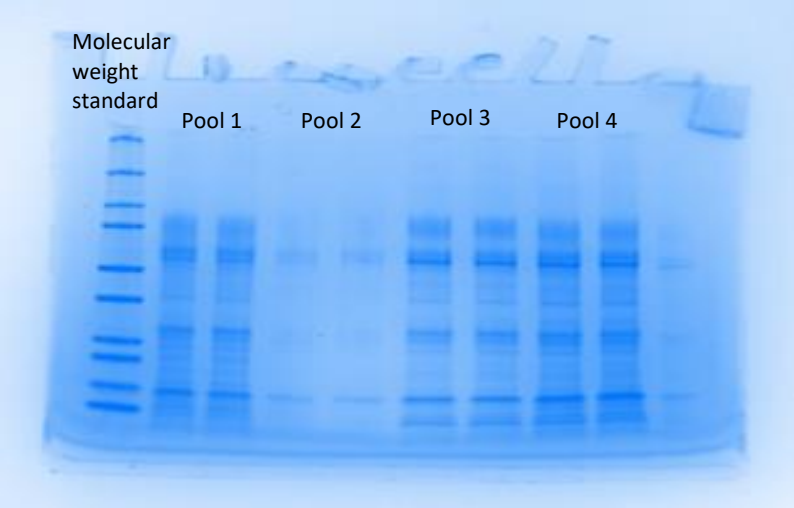

Figure 20. *The SDS-PAGE gel obtained in reducing and non-reducing conditions*

5 Discussion

Due to the restrictions deriving from the SARS-CoV-2 emergency, it was not possible to carry out the experiments using the biological fluids to be analyzed. A future goal will be to complete the experimental path to establish a correlation between genotype and salivary proteomic phenotype. The achievement of this objective could be important in the diagnostic field for the rapid and early discrimination of the various forms of porphyria.

Bibliography

1. Phillips, J. D. Heme biosynthesis and the porphyrias. *Mol. Genet. Metab.* **128**, 164–177 (2019).
2. Puy, H., Gouya, L. & Deybach, J.-C. Porphyrias. *Lancet* **375**, 924–937 (2010).
3. Biochemistry (3rd edn). C.K. Mathews, K.E. Van Holde, K.G. Ahern (eds). *Int. Microbiol.* (2001) doi:10.2436/im.v4i3.9330.
4. Fujiwara, T. & Harigae, H. Biology of Heme in Mammalian Erythroid Cells and Related Disorders. *Biomed Res. Int.* **2015**, 1–9 (2015).
5. Mohan, G. & Madan, A. *Ala Dehydratase Deficiency Porphyria*. *StatPearls* (2020).
6. Loskove, Y. *et al.* Acute hepatic porphyrias: Identification of 46 hydroxymethylbilane synthase, 11 coproporphyrinogen oxidase, and 20 protoporphyrinogen oxidase novel mutations. *Mol. Genet. Metab.* **128**, 352–357 (2019).
7. Stölzel, U., Kubisch, I. & Stauch, T. Porphyrien – was ist gesichert? *Internist (Berl).* **59**, 1239–1248 (2018).
8. Lannfelt, L. *et al.* Porphobilinogen deaminase in human erythrocytes: purification of two forms with apparent molecular weights of 40 kDa and 42 kDa. *Scand. J. Clin. Lab. Invest.* **49**, 677–684 (1989).
9. Louie, G. V. *et al.* Structure of porphobilinogen deaminase reveals a flexible multidomain polymerase with a single catalytic site. *Nature* **359**, 33–39 (1992).
10. D'Avola, D. *et al.* Phase I open label liver-directed gene therapy clinical trial for acute intermittent porphyria. *J. Hepatol.* **65**, 776–783 (2016).
11. Unzu, C. *et al.* Porphobilinogen deaminase over-expression in hepatocytes, but not in erythrocytes, prevents accumulation of toxic porphyrin precursors in a mouse model of acute intermittent porphyria. *J. Hepatol.* **52**, 417–424 (2010).
12. Elder, G. H. Genetic Defects in the Porphyrias: Types and Significance. *Clin. Dermatol.* **16**, 225–233 (1998).
13. Spiritos, Z., Salvador, S., Mosquera, D. & Wilder, J. Acute Intermittent Porphyria: Current Perspectives And Case Presentation. *Ther. Clin. Risk Manag.* **Volume 15**, 1443–1451 (2019).
14. Singal, A. K. & Anderson, K. E. *Variegate Porphyria*. *GeneReviews®* (1993).
15. MORGAN, R. R., ERRINGTON, R. & ELDER, G. H. Identification of sequences required for the import of human protoporphyrinogen oxidase to mitochondria. *Biochem. J.* **377**, 281–287 (2004).

16. TAKETANI, S. *et al.* The Human Protoporphyrinogen Oxidase Gene (PPOX): Organization and Location to Chromosome 1. *Genomics* **29**, 698–703 (1995).
17. Kooijman, M. M. D. & Brand, H. S. Oral aspects of porphyria. *Int. Dent. J.* **55**, 61–66 (2005).
18. van Tuyll van Serooskerken, A. M. *et al.* Digenic Inheritance of Mutations in the Coproporphyrinogen Oxidase and Protoporphyrinogen Oxidase Genes in a Unique Type of Porphyria. *J. Invest. Dermatol.* **131**, 2249–2254 (2011).
19. Wang, B. & Bissell, D. M. *Hereditary Coproporphyria*. *GeneReviews®* (1993).
20. Wiman, Å., Floderus, Y. & Harper, P. Two novel mutations and coexistence of the 991C.T and the 1339C.T mutation on a single allele in the coproporphyrinogen oxidase gene in Swedish patients with hereditary coproporphyria. *J. Hum. Genet.* **47**, 407–412 (2002).
21. Lamoril, J. *et al.* Characterization of Mutations in the CPO Gene in British Patients Demonstrates Absence of Genotype-Phenotype Correlation and Identifies Relationship between Hereditary Coproporphyria and Harderoporphyria. *Am. J. Hum. Genet.* **68**, 1130–1138 (2001).
22. Gitter, S. J., Cooper, C. L., Friesen, J. A. & Jones, M. A. Investigation of the catalytic and structural roles of conserved histidines of human coproporphyrinogen oxidase using site-directed mutagenesis. *Med. Sci. Monit.* **13**, BR1-10 (2007).
23. Schmitt, C. *et al.* Mutations in human CPO gene predict clinical expression of either hepatic hereditary coproporphyria or erythropoietic harderoporphyria. *Hum. Mol. Genet.* **14**, 3089–3098 (2005).
24. Aurizi, C. *et al.* Four novel mutations of the coproporphyrinogen III oxidase gene. *Cell. Mol. Biol. (Noisy-le-grand).* **55**, 15–8 (2009).
25. Borrero Corte, M. J. *et al.* Molecular analysis of 19 Spanish patients with mixed porphyrias. *Eur. J. Med. Genet.* **62**, 103589 (2019).
26. Doss, M. O. *et al.* The third case of Doss porphyria (δ-amino-levulinic acid dehydratase deficiency) in Germany. *J. Inherit. Metab. Dis.* **27**, 529–536 (2004).
27. Plewinska, M., Thunell, S., Holmberg, L., Wetmur, J. G. & Desnick, R. J. delta-Aminolevulinate dehydratase deficient porphyria: identification of the molecular lesions in a severely affected homozygote. *Am. J. Hum. Genet.* **49**, 167–74 (1991).
28. Madan, P. *et al.* Hans Gunther and his disease. *Photodermatol. Photoimmunol. Photomed.* **23**, 261–263 (2007).
29. Howard, M., Hall, A. & Ramsay, D. Congenital erythropoietic porphyria (Gunther disease) -

long-term follow up of a case and review. *Dermatol. Online J.* **23**, (2017).

30. Erwin, A. L. & Desnick, R. J. Congenital erythropoietic porphyria: Recent advances. *Mol. Genet. Metab.* **128**, 288–297 (2019).
31. Singal, A. K. Porphyria cutanea tarda: Recent update. *Mol. Genet. Metab.* **128**, 271–281 (2019).
32. Bleasel, N. R. & Varigos, G. A. Porphyria cutanea tarda. *Australas. J. Dermatol.* **41**, 197–208 (2000).
33. Méndez, M. *et al.* Molecular analysis of the UROD gene in 17 Argentinean patients with familial porphyria cutanea tarda: Characterization of four novel mutations. *Mol. Genet. Metab.* **105**, 629–633 (2012).
34. Ahmed jan, N. & Masood, S. *Erythropoietic Protoporphyria*. *StatPearls* (2020).
35. Di Pierro, E. *et al.* A 10376 bp deletion of FECH gene responsible for erythropoietic protoporphyria. *Blood Cells, Mol. Dis.* **40**, 233–236 (2008).
36. Long, Z. *et al.* Identification of FECH gene multiple variations in two Chinese patients with erythropoietic protoporphyria and a review. *J. Zhejiang Univ. B* **17**, 813–820 (2016).
37. Di Pierro, E., Brancaleoni, V., Moriondo, V., Besana, V. & Cappellini, M. Co-existence of two functional mutations on the same allele of the human ferrochelatase gene in erythropoietic protoporphyria. *Clin. Genet.* **71**, 84–88 (2006).
38. Lecha, M., Puy, H. & Deybach, J.-C. Erythropoietic protoporphyria. *Orphanet J. Rare Dis.* **4**, 19 (2009).
39. Balwani, M. Erythropoietic Protoporphyria and X-Linked Protoporphyria: pathophysiology, genetics, clinical manifestations, and management. *Mol. Genet. Metab.* **128**, 298–303 (2019).
40. Brancaleoni, V. *et al.* X-chromosomal inactivation directly influences the phenotypic manifestation of X-linked protoporphyria. *Clin. Genet.* **89**, 20–26 (2016).
41. Bishop, D. F., Henderson, A. S. & Astrin, K. H. Human δ-aminolevulinate synthase: Assignment of the housekeeping gene to 3p21 and the erythroid-specific gene to the X chromosome. *Genomics* **7**, 207–214 (1990).
42. Balwani, M., Desnick, R. & Porphyrias Consortium of the NIH-Sponsored Rare Diseases Clinical Research Network. *X-Linked Protoporphyria*. *GeneReviews®* (1993).
43. Stölzel, U., Doss, M. O. & Schuppan, D. Clinical Guide and Update on Porphyrias. *Gastroenterology* **157**, 365-381.e4 (2019).

44. Pedersen, A. M. L., Sørensen, C. E., Proctor, G. B., Carpenter, G. H. & Ekström, J. Salivary secretion in health and disease. *J. Oral Rehabil.* **45**, 730–746 (2018).
45. Humphrey, S. P. & Williamson, R. T. A review of saliva: normal composition, flow, and function. *J. Prosthet. Dent.* **85**, 162–9 (2001).
46. Campo-Deaño, L., Dullens, R. P. A., Aarts, D. G. A. L., Pinho, F. T. & Oliveira, M. S. N. Viscoelasticity of blood and viscoelastic blood analogues for use in polydymethylsiloxane in vitro models of the circulatory system. *Biomicrofluidics* **7**, 034102 (2013).
47. Blood Rheology and Hemodynamics. *Semin. Thromb. Hemost.* **29**, 435–450 (2003).
48. Nelson, D. L. & Cox, M. M. Lehninger Principles of Biochemistry 7th. *W.H. Free. Co.* (2017).
49. Cook, J. D., Caplan, Y. H., LoDico, C. P. & Bush, D. M. The Characterization of Human Urine for Specimen Validity Determination in Workplace Drug Testing: A Review. *J. Anal. Toxicol.* **24**, 579–588 (2000).
50. Maranda, E. L. *et al.* Porphyria and Vampirism—A Myth, Sensationalized. *JAMA Dermatology* **152**, 975 (2016).
51. Mlacker, S., Shah, V. V., Alsaidan, M. & Nouri, K. Victorian Vampires Validated—The Similarities Between a Legendary Creature and a Dermatologic Pathology. *JAMA Dermatology* **151**, 1225 (2015).
52. Cox, A. M. Porphyria and vampirism: another myth in the making. *Postgrad. Med. J.* **71**, 643–644 (1995).
53. Cox, T. M. *et al.* King George III and porphyria: an elemental hypothesis and investigation. *Lancet* **366**, 332–335 (2005).
54. Lorenzo-Pouso, A. I. *et al.* Protein-Based Salivary Profiles as Novel Biomarkers for Oral Diseases. *Dis. Markers* **2018**, 1–22 (2018).
55. Bruinsma, F. J., Joo, J. E., Wong, E. M., Giles, G. G. & Southey, M. C. The utility of DNA extracted from saliva for genome-wide molecular research platforms. *BMC Res. Notes* **11**, 8 (2018).
56. Guha, P., Das, A., Dutta, S. & Chaudhuri, T. K. A rapid and efficient DNA extraction protocol from fresh and frozen human blood samples. *J. Clin. Lab. Anal.* **32**, e22181 (2018).
57. Ule, J. & Blencowe, B. J. Alternative Splicing Regulatory Networks: Functions, Mechanisms, and Evolution. *Mol. Cell* **76**, 329–345 (2019).
58. Reece, J. B. *Campbell biology*. (2011).
59. Guillén-Navarro, E., Carbonell, P., Glover, G., Sánchez-Solís, M. & Fernández-Barreiro, A.

Novel HMBS founder mutation and significant intronic polymorphism in Spanish patients with acute intermittent porphyria. *Ann. Hum. Genet.* **68**, 509–514 (2004).

60. Mayr, C. Regulation by 3′-Untranslated Regions. *Annu. Rev. Genet.* **51**, 171–194 (2017).
61. Chatterjee, S. & Pal, J. K. Role of 5′- and 3′-untranslated regions of mRNAs in human diseases. *Biol. Cell* **101**, 251–262 (2009).
62. Lim, K. H., Ferraris, L., Filloux, M. E., Raphael, B. J. & Fairbrother, W. G. Using positional distribution to identify splicing elements and predict pre-mRNA processing defects in human genes. *Proc. Natl. Acad. Sci.* **108**, 11093–11098 (2011).
63. Strauss, B. S. Frameshift mutation, microsatellites and mismatch repair. *Mutat. Res. Mutat. Res.* **437**, 195–203 (1999).
64. Seligmann, H. & Pollock, D. D. The Ambush Hypothesis: Hidden Stop Codons Prevent Off-Frame Gene Reading. *DNA Cell Biol.* **23**, 701–705 (2004).
65. Sánchez-Soler, M. J., Barreda-Sánchez, M., Ballesta-Martínez, M. J., Glóver, G. & Guillén-Navarro, E. Acute intermittent porphyria in a paediatric population in the region of Murcia: Phenotype and prevalence. *An. Pediatría (English Ed.* **84**, 114–115 (2016).
66. Dreyer Gavin. Examining the urine--what can it tell us at the bed-side? *Malawi Med J* (2010).
67. Castelbón Fernández, F. J., Solares Fernandez, I., Arranz Canales, E., Enríquez de Salamanca Lorente, R. & Morales Conejo, M. Protocolo de actuación en pacientes con sospecha de porfiria aguda. *Rev. Clínica Española* **220**, 592–596 (2020).
68. Lang, A. *et al.* Rapid spectrophotometric quantification of urinary porphyrins and porphobilinogen as screening tool for attacks of acute porphyria. *J. Biomed. Opt.* **23**, 1 (2018).
69. Lamon, J. M., Frykholm, B. C. & Tschudy, D. P. Screening Tests in Acute Porphyria. *Arch. Neurol.* **34**, 709–712 (1977).
70. Llorente., J. J. N. M. V. G. del O. M. R. C.-S. R. B. D. O. S. S. D. C. N. R. E. de S. The power of the Hoesch test. (2016).
71. Szlendak, U., Bykowska, K. & Lipniacka, A. Clinical, Biochemical and Molecular Characteristics of the Main Types of Porphyria. *Adv. Clin. Exp. Med.* **25**, 361–368 (2016).
72. Kufner, G., Schlegel, H. & Jäger, R. A spectrophotometric micromethod for determining erythrocyte protoporphyrin-IX in whole blood or erythrocytes. *Clin. Chem. Lab. Med.* **43**, (2005).

73. Piomelli S. Free erythrocyte porphyrins in the detection of undue absorption of Pb and of Fe deficiency. *Clin. Chem.* (1977).
74. Ulbrichova, D. *et al.* Correlation between biochemical findings, structural and enzymatic abnormalities in mutated HMBS identified in six Israeli families with acute intermittent porphyria. *Blood Cells, Mol. Dis.* **42**, 167–173 (2009).
75. Hift, R. J., Davidson, B. P., van der Hooft, C., Meissner, D. M. & Meissner, P. N. Plasma Fluorescence Scanning and Fecal Porphyrin Analysis for the Diagnosis of Variegate Porphyria: Precise Determination of Sensitivity and Specificity with Detection of Protoporphyrinogen Oxidase Mutations as a Reference Standard. *Clin. Chem.* **50**, 915–923 (2004).
76. Aslam, B., Basit, M., Nisar, M. A., Khurshid, M. & Rasool, M. H. Proteomics: Technologies and Their Applications. *J. Chromatogr. Sci.* **55**, 182–196 (2017).
77. Cristea, I. M., Gaskell, S. J. & Whetton, A. D. Proteomics techniques and their application to hematology. *Blood* **103**, 3624–3634 (2004).
78. Cui, W., Rohrs, H. W. & Gross, M. L. Top-down mass spectrometry: Recent developments, applications and perspectives. *Analyst* **136**, 3854 (2011).
79. Addona, T. A. *et al.* A pipeline that integrates the discovery and verification of plasma protein biomarkers reveals candidate markers for cardiovascular disease. *Nat. Biotechnol.* **29**, 635–643 (2011).
80. Roi, A. *et al.* A New Approach for the Diagnosis of Systemic and Oral Diseases Based on Salivary Biomolecules. *Dis. Markers* **2019**, 1–11 (2019).
81. Castagnola, Massimo Scarano, E., Passali, G C, Messana, I, Cabras, T. Salivary biomarkers and proteomics: future diagnostic and clinical utilities. *Acta Otorhinolaryngol Ital.* (2017) doi:https://vpn.unica.it/https/doi.org/10.14639/0392-100x-1598.
82. Castagnola, M. *et al.* The human salivary proteome: a critical overview of the results obtained by different proteomic platforms. *Expert Rev. Proteomics* **9**, 33–46 (2012).
83. M., C. *et al.* Determination of the Post-Translational Modifications of Salivary Acidic Proline-Rich Proteins. *Eur. J. Morphol.* **41**, 93–98 (2003).
84. Inzitari, R. *et al.* Different isoforms and post-translational modifications of human salivary acidic proline-rich proteins. *Proteomics* **5**, 805–815 (2005).
85. Atzen E A, et all. PRB1, PRB2, and PRB4 coded polymorphisms among human salivary concanavalin-A binding, II-1, and Po proline-rich proteins. *Am J Hum Genet.* (1996)

doi:https://vpn.unica.it/https/www.ncbi.nlm.nih.gov/pubmed/8554050.

86. Manconi, B. *et al.* N- and O-linked glycosylation site profiling of the human basic salivary proline-rich protein 3M. *J. Sep. Sci.* **39**, 1987–1997 (2016).

87. Levine, M. J. *et al.* Structural Aspects of Salivary Glycoproteins. *J. Dent. Res.* **66**, 436–441 (1987).

88. Ployon, S. *et al.* Mechanisms of astringency: Structural alteration of the oral mucosal pellicle by dietary tannins and protective effect of bPRPs. *Food Chem.* **253**, 79–87 (2018).

89. Könönen, E., Kanervo, A., Takala, A., Asikainen, S. & Jousimies-Somer, H. Establishment of Oral Anaerobes during the First Year of Life. *J. Dent. Res.* **78**, 1634–1639 (1999).

90. Castagnola, M. *et al.* The Surprising Composition of the Salivary Proteome of Preterm Human Newborn. *Mol. Cell. Proteomics* **10**, M110.003467 (2011).

91. Hirtz, C. *et al.* MS characterization of multiple forms of alpha-amylase in human saliva. *Proteomics* **5**, 4597–4607 (2005).

92. Peyrot des Gachons, C. & Breslin, P. A. S. Salivary Amylase: Digestion and Metabolic Syndrome. *Curr. Diab. Rep.* **16**, 102 (2016).

93. Parkkila S et al. Salivary carbonic anhydrase protects gastroesophageal mucosa from acid injury. *Dig Dis Sci.* (1997) doi:10.1023/a:1018889120034.

94. Leinonen, J., Kivelä, J., Parkkila, S., Parkkila, A.-K. & Rajaniemi, H. Salivary Carbonic Anhydrase Isoenzyme VI Is Located in the Human Enamel Pellicle. *Caries Res.* **33**, 185–190 (1999).

95. Schroeder, H. W. & Cavacini, L. Structure and function of immunoglobulins. *J. Allergy Clin. Immunol.* **125**, S41–S52 (2010).

96. Fábián, T. K., Hermann, P., Beck, A., Fejérdy, P. & Fábián, G. Salivary Defense Proteins: Their Network and Role in Innate and Acquired Oral Immunity. *Int. J. Mol. Sci.* **13**, 4295–4320 (2012).

97. Fabian, T., Fejerdy, P. & Csermely, P. Salivary Genomics, Transcriptomics and Proteomics: The Emerging Concept of the Oral Ecosystem and their Use in the Early Diagnosis of Cancer and other Diseases. *Curr. Genomics* **9**, 11–21 (2008).

98. Frenkel, E. S. & Ribbeck, K. Salivary mucins in host defense and disease prevention. *J. Oral Microbiol.* **7**, 29759 (2015).

99. Turk, ">Vito. Cystatins: Biochemical and structural properties, and medical relevance. *Front. Biosci.* **Volume**, 5406 (2008).

100. Balbøn, M. *et al.* A sequence variation in the human cystatin D gene resulting in an amino acid (Cys/Arg) polymorphism at the protein level. *Hum. Genet.* **90**, (1993).
101. Lupi, A. *et al.* Identification of the human salivary cystatin complex by the coupling of high-performance liquid chromatography and ion-trap mass spectrometry. *Proteomics* **3**, 461–467 (2003).
102. Ahmad, M., Piludu, M., Oppenheim, F. G., Helmerhorst, E. J. & Hand, A. R. Immunocytochemical Localization of Histatins in Human Salivary Glands. *J. Histochem. Cytochem.* **52**, 361–370 (2004).
103. OPPENHEIM, F. G., SALIH, E., SIQUEIRA, W. L., ZHANG, W. & HELMERHORST, E. J. Salivary Proteome and Its Genetic Polymorphisms. *Ann. N. Y. Acad. Sci.* **1098**, 22–50 (2007).
104. Cabras, T. *et al.* Tyrosine Polysulfation of Human Salivary Histatin 1. A Post-Translational Modification Specific of the Submandibular Gland. *J. Proteome Res.* **6**, 2472–2480 (2007).
105. Castagnola, M. *et al.* A Cascade of 24 Histatins (Histatin 3 Fragments) in Human Saliva: SUGGESTIONS FOR A PRE-SECRETORY SEQUENTIAL CLEAVAGE PATHWAY. *J. Biol. Chem.* **279**, 41436–41443 (2004).
106. Driscoll, J. *et al.* Functional Comparison of Native and Recombinant Human Salivary Histatin 1. *J. Dent. Res.* **74**, 1837–1844 (1995).
107. Cabras, T. *et al.* HPLC–MS characterization of cyclo-statherin Q-37, a specific cyclization product of human salivary statherin generated by transglutaminase 2. *J. Sep. Sci.* **29**, 2600–2608 (2006).
108. P A Raj. Salivary statherin. Dependence on sequence, charge, hydrogen bonding potency, and helical conformation for adsorption to hydroxyapatite and inhibition of mineralization. *J Biol Chem.* (1992).
109. Messana, I. *et al.* Trafficking and Postsecretory Events Responsible for the Formation of Secreted Human Salivary Peptides. *Mol. Cell. Proteomics* **7**, 911–926 (2008).
110. Pisano, E. *et al.* Peptides of human gingival crevicular fluid determined by HPLC-ESI-MS. *Eur. J. Oral Sci.* **113**, 462–468 (2005).
111. Shafee, T. M. A., Lay, F. T., Phan, T. K., Anderson, M. A. & Hulett, M. D. Convergent evolution of defensin sequence, structure and function. *Cell. Mol. Life Sci.* **74**, 663–682 (2017).
112. Inzitari, R. *et al.* HPLC-ESI-MS analysis of oral human fluids reveals that gingival crevicular fluid is the main source of oral thymosins β 4 and β 10. *J. Sep. Sci.* **32**, 57–63 (2009).

113. Huff, T., Müller, C. S. ., Otto, A. M., Netzker, R. & Hannappel, E. β-Thymosins, small acidic peptides with multiple functions. *Int. J. Biochem. Cell Biol.* **33**, 205–220 (2001).
114. Marenholz, I., Heizmann, C. W. & Fritz, G. S100 proteins in mouse and man: from evolution to function and pathology (including an update of the nomenclature). *Biochem. Biophys. Res. Commun.* **322**, 1111–1122 (2004).
115. Abe, T. *et al.* Expression of the secretory leukoprotease inhibitor gene in epithelial cells. *J. Clin. Invest.* **87**, 2207–2215 (1991).
116. Sakaguchi, K. *et al.* Polymeric immunoglobulin receptor expression and local immunoglobulin A production in bovine sublingual, submandibular and parotid salivary glands. *Vet. J.* **197**, 291–296 (2013).
117. Martínez, A., Morales, R., Brethauer, U., Jiménez, M. & Alarcón, R. Porphyria cutanea tarda affecting lower lip. *Oral Surgery, Oral Med. Oral Pathol. Oral Radiol. Endodontology* **90**, 705–708 (2000).
118. Fayle, S. A. M. A. P. Congenital erythropoietic porphyria--oral manifestations and dental treatment in childhood: a case reporte.
119. Trodahl, J. N., Schwartz, S. & Gorlin, R. I. The pigmentation of dental tissues in erythropoietic (congenital) porphyria. *J. Oral Pathol. Med.* **1**, 159–171 (1972).